TOTAL SKIN ELECTRON IRRADIATION DOSIMETRY USING HIGH DOSE RATE MODE WITH A LINEAR ACCELERATOR AT RAMATHIBODI HOSPITAL

SUPAPORN SRISUWAN

A THESIS SUBMITTED IN PARTIAL FULFILLMENT
OF THE REQUIREMENTS FOR
THE DEGREE OF MASTER OF SCIENCE
(MEDICAL PHYSICS)
FACULTY OF GRADUATE STUDIES
MAHIDOL UNIVERSITY
2014

Thesis
entitled

TOTAL SKIN ELECTRON IRRADIATION DOSIMETRY USING HIGH DOSE RATE MODE WITH A LINEAR ACCELERATOR AT RAMATHIBODI HOSPITAL

Supaporn Srisuwan
.....
Miss Supaporn Srisuwan
Candidate

Puangpen Tangboonduangjit
.....
Lect. Puangpen Tangboonduangjit,
Ph.D. (Medical Radiation Physics)
Major advisor

Thiti Swangsilpa
.....
Assoc. Prof.Thiti Swangsilpa,
M.D.
Co-advisor

B. Mahaisavariya
.....
Prof. Banchong Mahaisavariya,
M.D., Dip Thai Board of Orthopedics
Dean
Faculty of Graduate Studies
Mahidol University

Puangpen Tangboonduangjit
.....
Lect. Puangpen Tangboonduangjit,
Ph.D. (Medical Radiation Physics)
Program Director
Master of Science Program in
Medical Physics
Faculty of Medicine
Ramathibodi Hospital
Mahidol University

Thesis
entitled

TOTAL SKIN ELECTRON IRRADIATION DOSIMETRY USING HIGH DOSE RATE MODE WITH A LINEAR ACCELERATOR AT RAMATHIBODI HOSPITAL

was submitted to the Faculty of Graduate Studies, Mahidol University
for the degree of Master of Science (Medical Physics)
on
March 26, 2014

Supaporn Srisuwan
.....
Miss Supaporn Srisuwan
Candidate

Sivalee Suriyapee
.....
Assoc. Prof. Sivalee Suriyapee,
M.Eng. (Nuclear Technology)
Chair

Puangpen Tangboonduangjit
.....
Lect. Puangpen Tangboonduangjit,
Ph.D. (Medical Radiation Physics)
Member

Thiti Swangsilpa
.....
Assoc. Prof.Thiti Swangsilpa,
M.D.
Member

B. Mahaisavariya
.....
Prof. Banchong Mahaisavariya,
M.D., Dip Thai Board of Orthopedics
Dean
Faculty of Graduate Studies
Mahidol University

.....
Prof. Winit Phuapradit,
M.D., M.P.H.
Dean
Faculty of Medicine
Ramathibodi Hospital,
Mahidol University

ACKNOWLEDGEMENTS

I would like to express my gratitude and deepest appreciation to my major advisor, Lect. Puangpen Tangboonduangjit for her knowledge, patience, motivation, and enthusiasm. Her guidance helped me in all the time of research and writing of this thesis, and the deepest appreciation to my co-advisor, Assist. Prof. Thiti Sawangsilp, M.D., Department of Radiology, Faculty of Medicine, Ramathibodi Hospital, Mahidol University for his kindness advice.

I would like to deeply thank to Assist. Prof. Chirapa Tannanonta, Radiation Oncology unit, Chulabhorn Hospital for her experience and kindness suggestion of research.

I would like to thank all staff in the Division of Radiation Oncology, Department of Radiology, Ramathibodi Hospital for their suggestion in the equipment usage on the measurement and a kindly support in many advices, and a specially thank to Miss Siwaporn Sakulsingharoj and Miss Daranee Piriyasang for their advice of the in vivo measurement.

A sincere thanks to my best fellow medical physic students, Miss Kawalee Rukthung, Miss Rattana Watjanon, Miss Supaporn Thongngam and Miss Viyada Sanoesan for their willingness to help me during the measurement.

I am also thankful to Master Science Program in Medical Physics, Faculty of Medicine Ramathibodi Hospital, Mahidol University, for supply the academic knowledge in Medical Physics.

I would like to express a grateful thank for funding support from the Graduate Studies of Mahidol University Alumni Association in my research.

Finally, I would also like to thank my family, my mother and my two sisters which supporting and encouraging me always with their best wishes.

Supaporn Srisuwan

TOTAL SKIN ELECTRON IRRADIATION DOSIMETRY USING HIGH DOSE RATE MODE WITH A LINEAR ACCELERATOR AT RAMATHIBODI HOSPITAL

SUPAPORN SRISUWAN 5236467 RAMP/M

M.Sc. (MEDICAL PHYSICS)

THESIS ADVISORY COMMITTEE: PUANGPEN TANGBOONDUANGJIT, Ph.D. (MEDICAL RADIATION PHYSICS), THITI SWANGSILPA, M.D.

ABSTRACT

The aim of this work was to verify dosimetric parameters for the TSEI technique following AAPM report 23 guideline by using the 6 MeV High Dose Rate Total skin electron Mode ($HDTse^{-}$) on a Varian Clinac iX linear accelerator. The technique is called Modified Stanford technique. The anthropomorphic phantom stands on a wooden treatment stand at a long SSD of 380 cm behind the large scatterer – degrader of 0.5 cm thickness and was irradiated with a combination of large dual gantry angle fields. The optimal tilt angle ($90^{\circ} \pm \theta$) was determined by verifying the vertical beam flatness along the matching beams. 2D dose distribution on treatment plane was performed by TLDs. Depth dose distribution was performed using Roos chamber and EBT2 film. The calibration point dose was measured by Roos chamber embeded on solid water phantoms at d_{max}. For the six dual angle field beams, the treatment skin dose was measured on a cylindrical phantom using TLDs taped at the point related to the calibration point dose using the overlapping factor B. The depth dose distribution was verified using the EBT2 film placed on slabs of anthropomorphic phantom. The dose uniformity was evaluated by using TLD-100 chips taped on the surface of anthropomorphic phantom at various locations. The results for the dual angle beams, the optimal tilt angle were found at ± 18°. The relative dose distribution in area of 180 x 80 cm^2 was 95% ± 6 %. The mean energy and the most probable energy were 3.3 MeV and 4.1 MeV, respectively. The depth dose distribution using Roos chamber matched that of using film. For six dual field beams, the overlapping factor B was 2.69. The maximum dose was shifted to the surface. R50 was 12 mm. The x-ray contamination was about 2 %. The dose uniformity on anthropomorphic phantom body surface was within ±10% of the prescribed dose. In conclusion, the dosimetric parameters met the requirement for TSEI treatment. The in vivo dosimetry is an important procedure to verify the dose uniformity around the patient's surface which is the main objective of the treatment.

KEY WORDS: TOTAL SKIN ELECTRON IRRADIATION / HIGH DOSE RATE TOTAL SKIN ELECTRON MODE / MODIFIED STANFORD TECHNIQUE

87 pages

การตรวจวัดข้อมูลทางรังสีสำหรับเทคนิคการฉายทั่วผิวหนังด้วยลำรังสีอิเล็กตรอนโดยใช้โหมดอัตราปริมาณรังสีต่อเวลาสูงของเครื่องเร่งอนุภาคโรงพยาบาลรามาธิบดี

TOTAL SKIN ELECTRON IRRADIATION DOSIMETRY USING HIHG DOSE RATE MODE WITH A LINEAR ACCELERATOR AT RAMATHIBODI HOSPITAL

สุภาพร ศรีสุวรรณ 5236467 RAMP/M

วท.ม. (ฟิสิกส์การแพทย์)

คณะกรรมการที่ปรึกษาวิทยานิพนธ์ : พวงเพ็ญ ตั้งบุญดวงจิตร, Ph.D.(MEDICAL RADIATION PHYSICS),
ธิติ สว่างศิลป์ M.D.

บทคัดย่อ

วัตถุประสงค์ของงานนี้คือทำการตรวจสอบข้อมูลทางรังสีสำหรับเทคนิคการฉายทั่วผิวหนังด้วยลำอิเล็กตรอนตามแนวทางปฏิบัติใน AAPM REPORT 23 โดยใช้อิเล็กตรอนพลังงาน 6 MeVโหมดอัตราปริมาณรังสีต่อเวลาสูงของเครื่องเร่งอนุภาคโรงพยาบาลรามาธิบดี เทคนิคการฉายที่ใช้คือ Modified Standford technique โดยหุ่นจำลองยืนบนอุปกรณ์ทำด้วยไม้ที่ระยะห่างจากแหล่งกำเนิดรังสี 380 ซม. อยู่หลังแผ่นกระเจิงและลดทอนพลังงานขนาดใหญ่ความหนา 0.5 ซม. ฉายด้วยลำรังสีขนาดใหญ่ที่ได้จากการยกทิศทางหัวเครื่องฉายรังสีทำมุมขึ้นและลงจากแนวระนาบ (90°±Θ) โดยมุมที่เหมาะสมหาได้จากการตรวจสอบความสม่ำเสมอของปริมาณรังสีในแนวความสูง จากนั้นจึงตรวจสอบการกระจายของปริมาณรังสีในแนวสองมิติของพื้นที่ลำรังสีขนาดใหญ่ด้วยทีแอลดี การวัดปริมาณรังสีที่ความลึกต่างๆทำโดยใช้ Roos chamber กับฟิล์ม การวัดปริมาณรังสีของตำแหน่ง Calibration โดยใช้ Roos chamber วางไว้ที่วัสดุที่มีความหนาเทียบเท่ากับน้ำโดยอยู่ที่ความลึกที่ให้ปริมาณรังสีสุด สำหรับการวัดส่วนการเข้าของลำรังสีหกทิศทางโดยทำการวัดปริมาณรังสีเฉลี่ยที่ผิวรอบหุ่นจำลองทรงกระบอกด้วยทีแอลดีซึ่งสัมพันธ์กับปริมาณรังสีที่ตำแหน่ง Calibration ด้วยค่า overlapping factor B การวัดปริมาณรังสีที่ความลึกต่างๆทำโดยใช้ฟิล์มวางระหว่างชั้นของหุ่นจำลองรูปร่างและโครงสร้างเหมือนมนุษย์ ความสม่ำเสมอของปริมาณรังสีที่ผิวทำได้โดยติดทีแอลดีบนผิวของหุ่นจำลองที่ตำแหน่งต่างๆ ผลที่ได้ของมุมที่เหมาะสมคือการยกทิศทางหัวเครื่องฉายรังสีทำมุมขึ้นและลงจากแนวระนาบ ± 18° การกระจายของปริมาณรังสีในแนวสองมิติของพื้นที่ลำรังสีขนาดใหญ่ 180 × 80 ตารางเซนติเมตร มีค่า 95% ± 6 %, ค่าพลังงานเฉลี่ยและค่าพลังงานสูงสุดมีค่า 3.3 MeV และ 4.1 MeV ตามลำดับ ผลของการวัดปริมาณรังสีที่ความลึกต่างๆทำโดยใช้ Roos chamber ได้ค่าสอดคล้องกับการวัดด้วยฟิล์ม สำหรับผลของการวัดในการเข้าของลำรังสีหกทิศทาง ได้ค่า overlapping factor B เท่ากับ 2.69 ค่าปริมาณรังสีสูงสุดขยับมาอยู่ที่ผิว ค่าปริมาณรังสีครึ่งหนึ่งของค่าปริมาณรังสีสูงสุดอยู่ที่ระยะ 12 มิลลิเมตร ค่า x- ray contamination มีค่าประมาณ 2 % ค่าความสม่ำเสมอของปริมาณรังสีที่ผิวของหุ่นจำลองมีค่าอยู่ในช่วง ± 10% ของปริมาณรังสีที่ให้ สรุปได้ว่าข้อมูลทางรังสีที่ได้สอดคล้องกับสิ่งที่เทคนิคการฉายนี้ต้องการ การวัดปริมาณรังสีในผู้ป่วยขณะทำฉายเป็นส่วนที่สำคัญเพื่อเป็นการตรวจ สอบความสม่ำเสมอของปริมาณรังสีที่ผู้ป่วยได้รับซึ่งเป็นวัตถุประสงค์หลักของการรักษา

87 หน้า

CONTENTS

LIST OF TABLES

LIST OF FIGURES

LIST OF FIGURES (cont.)

LIST OF FIGURES (cont.)

LIST OF ABBREVIATIONS

Abbreviations	Term
a	The accelerator's window
AAPM	American Association of Physicists in Medicine
cGy	Centigray
cm	Centimeter
cm^2	Square centimeter
^oC	Degree Celsius
c_{pl}	Depth scaling factor
D_d	The absorbed dose at any depth
D_m	The maximum absorbed dose
D_s	The surface absorbed dose
$D_{w,Q}$	Absorbed dose to water at the reference depth in a water phantom irradiated by a beam quality of Q
D_x	The x-ray contamination dose
$\bar{E}$	The mean energy in an electron beam
$\bar{E}_0$, $\bar{E}_z$	The mean electron energy at the phantom surfaceand at depth z
E_m	The maximum energy in an electron beam
E_p	The most probable energy in an electron beam
$E_{p,a}$,$E_{p,0}$,$E_{p,z}$	The most probable energy at the accelerator exit window, phantom surface and at depth z
EBT2	External Beam Therapy 2
ECC_i	The Element Correction Coefficient
EPID	Electronic portal imaging device
EORTC	The European Organization for Research and Treatment of Cancer
g/cm^2	Gram per square centimeter

LIST OF ABBREVIATIONS (cont.)

Abbreviations	Term
g/cm^3	Gram per cubic centimeter
$HDTse^-$	High Dose Rate Total skin electron Mode
h_{pl}	Fluence - scaling factor
IAEA	International Atomic Energy Agency
ICRU	International Commission on Radiation Units and Measurements
k_{elec}	Calibrator factor of an electrometer
k_Q	Chamber specific factor
k_{pol}	Polarity correction factor
k_s	Recombination correction factor
k_{TP}	Temperature pressure correction factor
MeV	Mega electron Volt
MF	Mycosis fungoides
M_Q	Reading of the dosimeter at the Quality Q
MU	Monitor Unit
nC	Nanocoulomb
N_{D,w,Q_0}	The absorbed dose to water calibration factor for a dosimeter at a reference beam
PDD	Percentage depth dose
$\bar{Q}$	Average charge of all TLDs
Q_{ci}	Corrected charge integral of standard TLD
Qi	Individual charge of each TLD
RCF	Reader calibration factor
R_{50}	The half- value of depth dose distribution in
R_p	The Practical range
SSD	Source to surface distance
$S_{w,air}$	Stopping power ratio from water to air

LIST OF ABBREVIATIONS (cont.)

Abbreviations	Term
TBI	Total Body Irradiation
TLD	Thermoluminiscence dosimeter
TSEI	Total Skin Electron Irradiation
V	Voltage
z_{max}	Depth of maximum dose
z_{ref}	Reference depth for in phantom measurement

CHAPTER I
INTRODUCTION

Total skin electron irradiation (TSEI) or Total skin electron therapy (TSET) is a special treatment technique in radiotherapy that use low energy electron beam 2 – 9 MeV for the treatment of skin lesion such as mycosis fungoides (MF), lymphoma cutis and karposi sarcoma. The superficial lesion is extending about 1 cm depth can be effectively treated without exceeding bone marrow tolerance[1]. This technique has been used since the 1960s which replaced kilovoltage x-ray treatment. Its objective is a delivery of uniform dose on the patient's skin with maximum dose at skin or near skin and minimum x-ray contamination in order to reduce harmful underneath organs and bone marrow toxicity. Characteristics of the electron beam are high surface dose, well defined range and rapid dose fall off at a depth beyond depth of maximum dose that there are consistent with the objective of treatment.

Mycosis fungoides, a cutaneous T –cell lymphoma treatment is the main use of this special technique. The malignant cells of MF are radiosensitive cells and effectively killed by a low dose of radiotherapy. The European Organization for Research and Treatment of Cancer (EORTC) has reached a consensus guidelines on clinical indications for TSEI in the management of MF[2]. The total treatment dose is usually 30 – 36 Gy over a period 8 – 10 weeks. Electron energy use depending on the penetration depth requirement or skin involvement of disease. TSEI is not widely use. It is in a few major centers because of the small incident of MF (4.5 per million people each year [3] and the requirements of this technique such as large field size, high surface dose with limited depth of penetration and surface dose uniformity. These are resulting in a complexity of implementation technique. In treatment, there are long treatment set-up and time. The treatment technique and dosimetry for implementation TSEI technique are reviewed in AAPM report 23, 1987[4].

1.1 Electron Beam

Electron beam has been used since the early 1950s in radiotherapy . The firstly was a Van der Graff generator with low electron energies. The development of a linear accelerator that generate photon and high electron energy were useful in radiotherapy. The application of electron in radiotherapy are treatment of skin cancers , chest wall irradiation in breast cancer , lymph node boost, and head and neck cancer.

1.1.1 Electron beam production

Clinical linac has electron energies range from 6 – 30 MeV [1]. Electron producing from electron gun are accelerated in the waveguide to the desired kinetic energy in a form of pencil beam that unsuitable for clinical use. It has two methods to boarden and flattening beam , The first method is scattering foil system that consists of a thin metallic foil (lead). When electron pencil beam strikes scattering foil , the beam has broadening and uniformity across treatment field. The second is scanning magnet that electron pencil beam is scanned across the field in a raster pattern using magnet control. Most linacs use scattering foil system as shown in Figure 1.1.

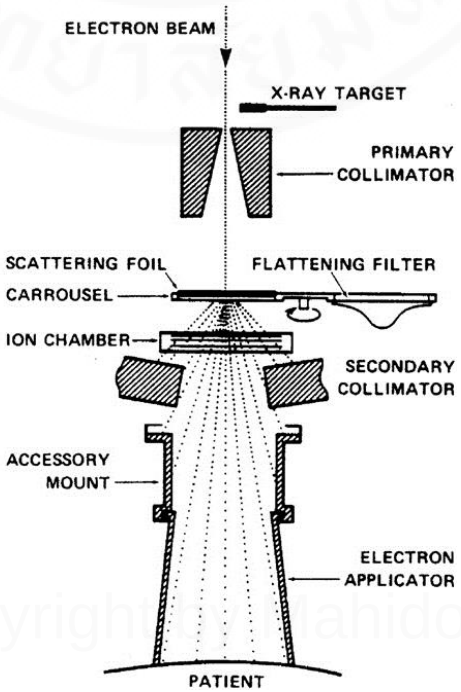

Figure 1.1 Electron beam production using the scattering foil system.

1.1.2 Energy parameter of the electron beam

Fig 1.2 shows electron beam parameters for 3 different locations on along the accelerator system; accelerator's window (a), the phantom surface (0) and depth in the phantom (z)[5]. The electron energy spectrum before strikes the accelerator's window is almost monoenergetic. When it passes through the exit window, scattering foil, monitor chamber and air results in energy loss and broadening of the electron spectrum. The energy at peak of the curve is characterized by most probable energy at the surface $E_{p,0}$ and a smaller energy is called mean energy at the surface $\bar{E}_0$. In clinical, these two energies at the phantom surface are used in the specification of the absorbed dose distribution and in selection of correction coefficients for dose measurements. As the electron beam passes through phantom, the energy becomes lower and spectrum becomes boarder.

The energy parameters are characterized by maximum energy $E_{m,}$ most probable energy $E_{p,}$ and mean energy $\bar{E}$. Additional subscripts are added to these parameters refer to 3 different locations.

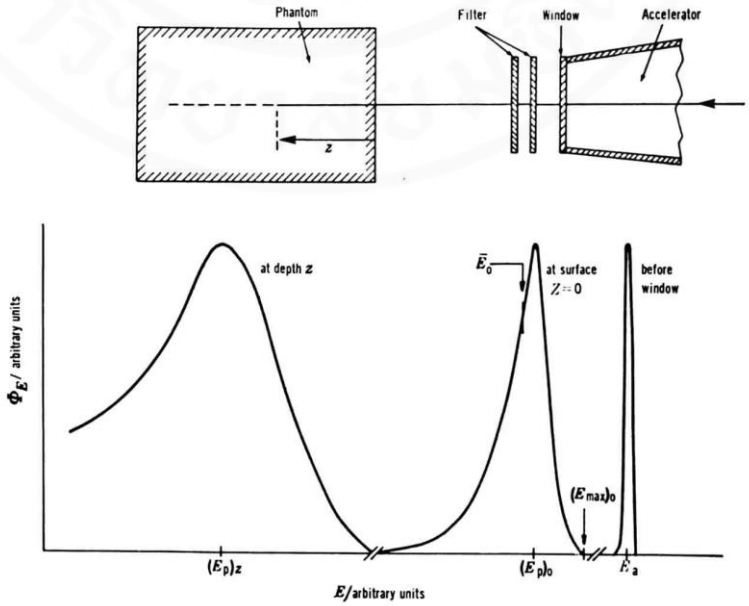

Figure 1.2 Electron beam parameter for 3 different locations.

1.1.3 Central Axis Depth Dose

Central axis depth dose is obtained by measuring the radiation distribution along the central axis of the beam as a function of depth in a homogenous, unit density phantom. The surface dose is high and then build up to a maximum as depth called depth of maximum dose $z_{max.}$ The dose drops rapidly beyond z_{max} to a low level dose called the bremsstrahlung tail. Figure 1.3 shows several parameters on central axis depth dose curve [6]. The surface dose, D_s, is absorbed dose on surface which is defined at 0.5 mm from surface because it is difficult to obtain accurate dose at air- phantom interface and this depth is the sensitive layer of epidermis. $D_{x,}$ is the x-ray contamination dose or bremsstrahlung. The therapeutic range R_t , is the depth of 90% absorbed dose beyond $z_{max.}$ The depth of the dose maximum R_{100}. The half value depth, R_{50} is the depth of 50% absorbed dose. The practical range, R_p is the depth at which the tangent to the curve at the point of inflection meet the level of D_m. R_{50} and R_p are used in a range of energy determination.

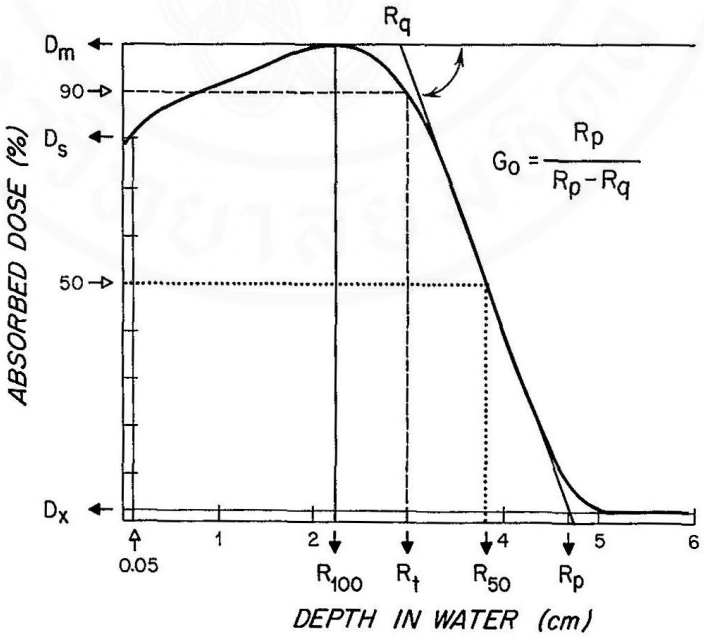

Figure 1.3 Central axis depth dose curve with the parameters used for characterize the electron beam.

1.1.4 Energy determination

The most probable energy, $E_{p,0}$ on the phantom surface is related to $R_{p,}$ the practical range in water as follows [6] :

$$E_{p,0} = C_1 + C_2 R_p + C_3 R_p^2 \quad (1)$$

Where R_p is the practical range in centimeter as defined in Figure 1.3
For water, C_1 = 0.22 MeV, C_2 = 1.98 MeV cm^{-1} and C_3 = 0.0025 MeV cm^{-2}

The mean electron energy, $\bar{E}_0$ at the phantom surface is related to the R_{50} as follows:

$$\bar{E}_0 = CR_{50} \quad (2)$$

Where C = 2.33 MeV/cm for water.

IAEA TRS 398 [7] specified the beam quality index in electron beam dosimetry with the half value depth R_{50}. The $R_{50,ion}$ is the half value of depth ionization distribution in water which the ionization current is 50% of its maximum value, The R_{50} is related to $R_{50,ion}$ as follows:

$$R_{50} = 1.029R_{50,ion} - 0.06 \ (g/cm^2) \qquad (\text{for } R_{50,ion} \le 10 \ g/cm^2) \quad (3)$$

$$R_{50} = 1.059R_{50,ion} - 0.37 \ (g/cm^2) \qquad (\text{for } R_{50,ion} \le 10 \ g/cm^2) \quad (4)$$

The mean energy at any depth z, $\bar{E}_z$ in a water phantom is related to the practical R_p as follows:

$$\bar{E}_z = \bar{E}_0 \ (1 - z/R_p) \quad (5)$$

1.1.5 Electron dosimetry

Electron dosimetry are devided into two categories: absolute dose measurement and relative dose distribution. Absolute dose measurement is used for defined absorbed dose at a reference point in phantom and a reference field size . Relative dose distribution is used for determination of depth dose curve, off-axis profiles and isodose distribution. Calorimetry, Fricky dosimeter and ionization chamber are used for determination of absorbed dose. Calorimetry is the most basic method for determination but is not practical in clinical setting due to the difficult of technique. The two latter dosimeters are most commonly used. Thermoluminescent dosimeters (TLD), film, and silicon diodes are used for determination of relative dose but not use for absolute dose measurement.

1.1.5.1 Ionization chamber

Ionization chamber has been used both for absolute and relative dose measurement. Ionization chamber is a gas - filled detector, usually air in a sensitive volume between two electrodes which are applied by voltage. The interaction of radiation ionized gas and electric field cause positive charges and low energy electrons in sensitive volume. Low energy electron attaches to a negative oxygen molecule in the air forming negative ions. Positive ion and negative ion are called ion pairs which move toward the electrodes of opposite sign and make the current or charge that can be measured by the electrometer. Chambers are designed in several geometries such as cylindrical, parallel-plate and spherical. The parallel-plate ion chambers are recommended for electron beam energies below 10 MeV in order to minimize scattering perturbation effect. The spacing of electrode is small (~2 mm) that minimizes cavity perturbation. Surface measurement is used practically due to thin window that has been eliminated significant wall attenuation. It is also suitable for measurement of depth dose along build- up region.

1.1.5.2 Thermoluminescence dosimeters (TLD)

Thermoluminescence is the phenomenon of light emission cause by heating imperfect crystal that absorbs ionizing radiation. The mechanisms of thermoluminescence show by energy stage of TL material in Figure 1.4 When the TL material is irradiated, The free electrons and holes occur in the TL material. The free electrons travel to the conduction band. They may be trapped in a metastable energy state or recombine with holes in the valence band (called fluorescence). They may be captured in trap for prolonged periods due to impurity in the crystal. When the TL material is heated the electrons are released from traps and emission of visible light. The emitted light is proportional to the absorbed dose that is detected by a photomultipler tube. TL material in radiation dosimetry includes Calcium sulfate ($CaSo_4$), Lithium fluoride (LiF) and Calcium fluoride (CaF_2) TL detectors obtained by doping phosphors with impurities called activators. Most commonly used is LiF:Mg-Ti (lithium fluoride doped with magnesium and titanium) because of their tissue equivalence (z_{eff} = 8.2). TLDs have various forms such as chips, powder, ribbons and rods. They are reusable and no cable required. High sensitivity can construction in small sizes that can be used in the body cavity and areas of high dose gradients such as buildup region. They are dose-rate independent. It has also been used for in vivo dosimetry. Theirs dose range are 10^{-5} to 10^{3} Gy.

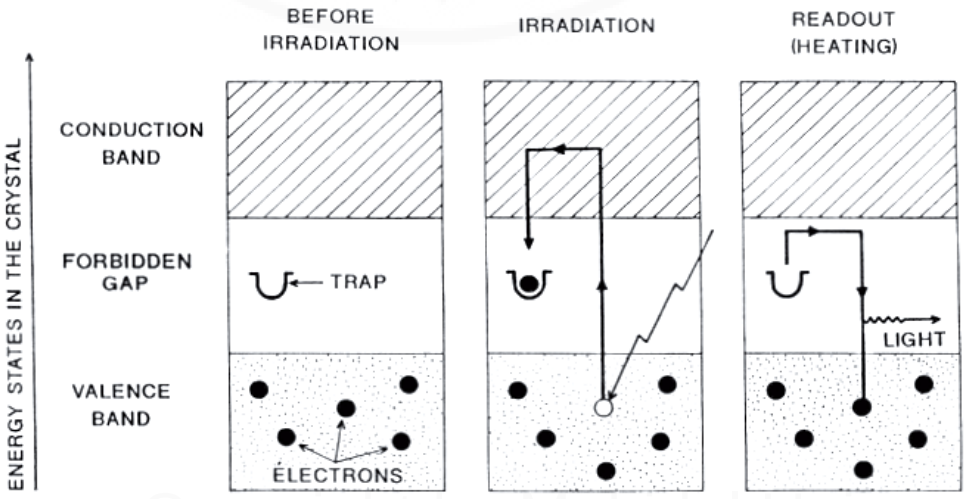

Figure 1.4 Energy stage of TL material**.**

1.1.5.3 Film dosimetry

Film has been used to measure dose distributions of electron beam with a convenient and rapid measurement. Radiographic film consists of a sensitive emulsion (AgBr) grains coated on thin plastic base. When film is irradiated , radiation interaction has changed chemical form of AgBr grains and produces latent image. It can be visible by chemical development called film processing (Developing, fixing and washing). Film opacity after irradiation and processing is proportional to dose. It can be determined by light transmission called optical density (OD). The instrument used to measure the optical density of a film is called a film densitometer. The OD is defined by

$$OD = \log_{10}\left(\frac{I_0}{I}\right) \tag{6}$$

Where I_o is the initial light intensity.

I is the transmitted light intensity through the film.

The relation between dose and OD are represented by sensitometric curve (characteristic or H&D curve) This is done by exposing film to a range of known doses, then plotting curve between the OD and dose. Sensitrometric curve must be done to cover a linear response of measured dose for the same batch and the same time.

The new type of film in radiotherapy dosimetry called Radiochromic film. It is also called GafChromic film that most commonly used in dosimetry. The components of radiochromic film are different from radiographic film. It is a self-developing film. When film is irradiated, the polymerization of sensitive component (dye) has occured in film. The polymer absorbs light. The densitometer is used to measure the transmission of light through the film. It is self-developing, no need of film processing. It is grainless which has a very high resolution and can be used in high dose gradient regions. The Advantages over radiographic films; is near-tissue equivalent (Z_{eff} = 6.84), dose rate independence, energy independence and insensitivity to ambient condition.

1.1.5.4 Semiconductor diode

Diodes are made of crystalline material such as silicon or germanium. Their atomic electrons are arranged in energy band. When the crystalline material is irradiated, electron–hole pairs are created. Electron move in the conduction band and motion of hole states in the valence band then producing an electrical pulse. It can be devided in donor or acceptor type by doping impurities material in to crystal such as acenic, phosphorus or boron. N-type diode has more electron in crystal (adding donor impurity). P-type diode has less electron in the crystal (adding acceptor impurity)

Silicon doped with boron (p-type diode) is most commonly use due to it has less radiation damage effect a smaller dark current. Fig 1.5 Shows principle of diode detection. When the diode is irradiated, The depletion layer will occur free electrons and holes. The electron was attracted to the positive side while the hole was attracted to the negative side of the diode, respectively. A signal current (I) is proportional to the number of charges.

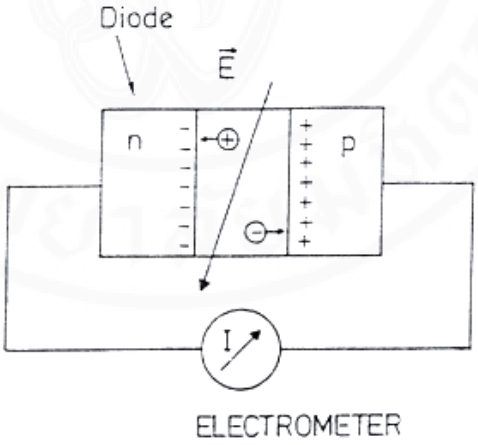

Figure 1.5 Principle of diode detection.

The advantage of diode are a good spatial resolution, a high sensitivity within a small volume, and a real-time response. It is widely used for in vivo dosimetry with real time readout but need a calibration before use. The disadvantage of diodes are temperature dependance, dose rate dependence, angular (directional) dependence and energy dependence.

1.2 Mycosis fungoides (MF)

It is the most common form of cutaneous T – cell lymphoma (CTCL), a type of non-Hodgkin's lymphoma. It was first described by Jean - Louis – Marc Alibert, French dermatologist in 1806. So it also called as Alibert – Bazin syndrome. The name of fungoides is unrelated to fungal infection but it derives from the characteristic of lesion that look like a mushroom. The cause of MF is unknown. There are many theories on causes. These include genetic, exposure to chemicals and infection agent. The Annual incidences are three new cases per million people each year in the united states. The median age is 56 years old. An occurrence in male was more than twice in female. The African - Americans had more twice incidence than Caucasians. The visible symptoms of patient present with patch, plaque limited to the skin, skin tumors or erythroderma (Sezary syndrome) involvement on the skin. Generally, MF is an indolent malignancy, with slow progression over years to decades. It can be misdiagnosis due to skin symptom lookalike dermatitis or fungal infection. The diagnosis is made by skin biopsy and confirm with blood or lymph nodes test [8].Treatment selection is based on prognostic factors, TMNB classification and overall clinical stage. Skin – directed therapies such as topical steroids, ultraviolet B, topical mechlorethamine, carmustine, psoralenplus ultraviolet A (PUVA) and Total skin electron irradiation (TSEI). Systemic therapies such as chemotherapy, steroids, retinoids, interferons. For TSEI, the patient with stage 1A and T1N1 disease may be treated with this technique. The pathologic remission was about 95%. EORTC recommended that the 80% isodose surface should be at least 4 mm deep to the skin surface and the dose at 20 mm deep should not be exceed 20% of maximum dose. Mycosis fungoides cell is radiosensitive cell which the alpha beta ratio is greater than 10 [9]. Ionizing radiation has been used in mycosis fungoides treatment since 1902, Scholtz [10] first used with low energy x-ray. The treatment was done in a small field ("spot"). It occurred ineffective result due to extension of disease out –side treatment field. In 1939, Sommerville [11] suggested a total skin x – ray both radiation, it was highly effective but the complication was severe.

The upcoming of electron beam therapy in 1950s which had an ideal range of penetration. The modification technique to treat large areas of lesion covering whole patient surface had been used in nowadays.

1.3 Development of total skin electron irradiation

The electron energies range from 2-9 MeV have been suggested for MF treatment due to the characteristic of the electron beam which high surface dose and a rapid fall off of depth beyond depth of maximum dose result in sparing of underneath tissue. TSEI has been developed over several decades. In 1953 Trump et al.[12] First used collimated 2.5 MeV electron beam generated from a Van der graft generator at a recumbent patient lying on a motorized table. The development of a medical linear accelerator was facilitated many institutes to use TSEI. Firstly, use the linear accelerator for TSEI technique at Stanford university [13]. Patient stood 10 feet from accelerator treatment head with gantry angle ±20 ° above and below the horizontal plane. A thin aluminum plate was placed at the end of treatment head to reduce electron energy and scatter electron for a result in beam uniformity at treatment plane. The original technique used four positions, anterior, posterior and two lateral opposing. A six field technique or a modification of the Standford technique had been replaced for a more uniform surface dose [14]. Six patient positions were anterior, posterior and four oblique as shown in Figure 1.7. This technique is most widely used in many institutes until today.

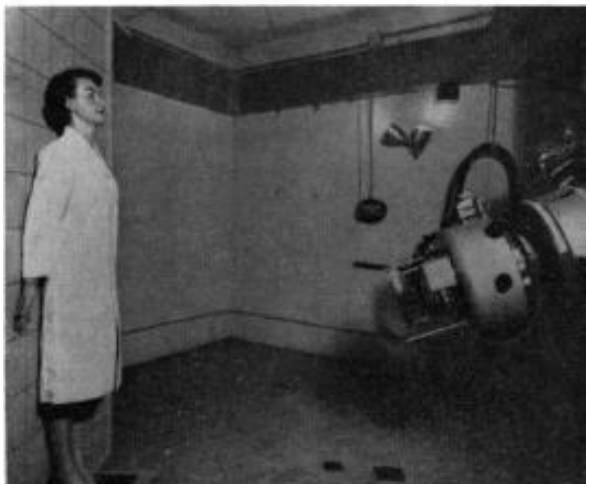

Figure 1.6 Treatment set up by Stanford medical linear accelerator.

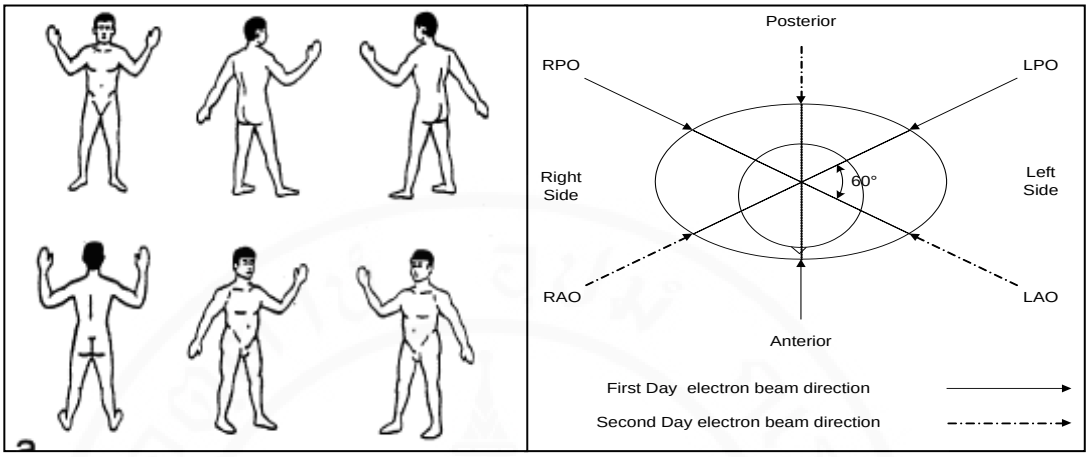

Figure 1.7 Six patient positions of Modified Stanford technique.

In 1978 Kumar et al. [15] described a rotational technique for better uniform dose distribution over the entire surface. Patient stood on a rotating platform with single field technique and rotates during the treatment. This technique can reduce set up and treatment time. Both Stanford technique and rotational technique were treating on a standing patient. The translation technique is the alternative technique which used lying on patient on a special treatment couch moving along fixed electron beam [16].

Some institutions had been adapted their technique such as lying on technique which patient laid on the floor and treating with six dual field technique [17]. The patient lying on a homemade rotating board which supporting during the treatment with six dual field technique[18]. Some institute had modified technique at a short treatment room by using three beam angulation instead of dual angle beam of Modified Standford technique [19]. Selection of TSEI technique depends on size of the treatment room and availability of equipment and facility at each institute.

Current total skin electron irradiation technique

The TSEI technique can be grouped into three techniques [20].

1. Translation technique

The patient lies on a special constructed couch which is translated through an electron beam (1.5 – 2 m SSD). The beam width is sufficient to cover transverse dimension of the patient.

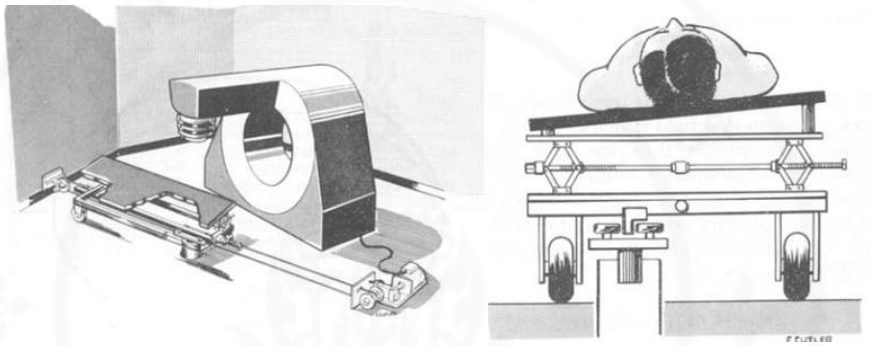

a. b.

Figure 1.8 Translation technique a. moving couch in a longitudinal direction b. The patient lays-on an adjustable couch.

2. Large electron field technique

A standing patient is treated at a large SSD with a single large electron beam (~ 7 m SSD) or a combination of large electron beam (3-4 m SSD). The latter is also known as dual angle field technique or Modified Stanford technique.

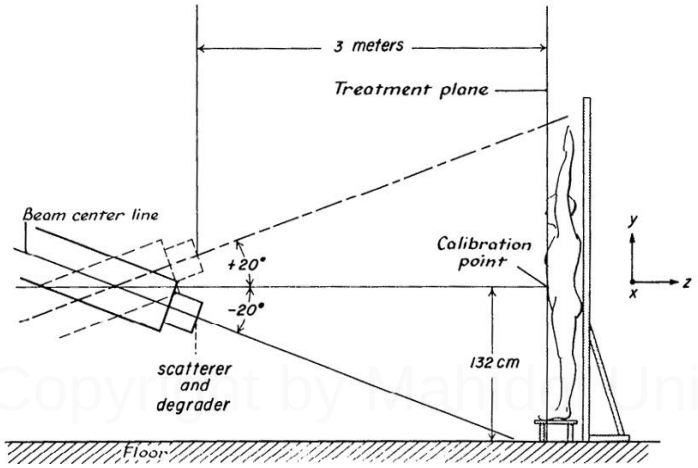

Figure 1.9 Large electron field technique.

3. Rotation technique

A large electron field technique which a patient rotates on platform controlled by the motor during irradiation, a scattering filter is inserted on the head of the gantry to optimize the beam uniformity [21].

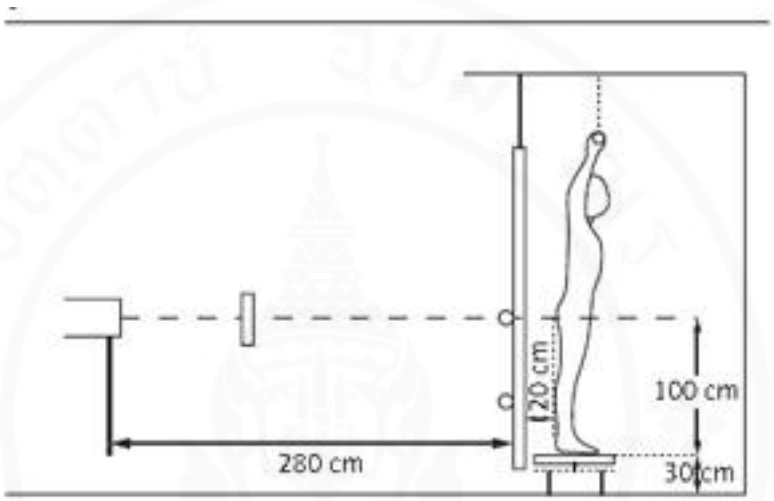

Figure 1.10 Rotational technique.

Physical requirements for total skin electron irradiation

There are several requirements to obtain the objective of TSEI treatment. The commissioning technique is concerning following them.

1. Electron field flatness

The electron field size at the treatment plane must cover patient from head to foot with a beam uniformity. AAPM23 recommended that the field size must be cover 200 cm x 80 cm. The vertical uniformity along superior to inferior is ± 8% and a horizontal uniformity is ± 4 % over 160 cm x 60 cm of treatment plane area. Large field size is obtained by using long SSD (3-7 m). The combination of beam angulation from horizontal ± 10º–20º can improve dose uniformity along the patient and most commonly use due to size of the treatment room. It can be used in 3- 4 m SSD for this technique. The dose distribution around the patient is improved by the use of multiple overlapping field (four - fields, six -fields, eight- fields, twelve fields) or rotational.

2. Electron beam energy

The electron beam energy from a linear accelerator range 6 – 10 MeV is used for this technique. It can be reduced to 3–7 MeV on the patient surface with the addition of the low Z transparent screen (polystyrene, lucite) called scatter - degrader 5–10 mm thickness, in front of the patient. The required penetration depth is upon the stage and type of disease. A penetration depth ranges from 5 mm to 15 mm or more of the 50% isodose surface which cover most lesions [4]. Scatter degrader is placed near the accelerator exit window or in front of the patient surface 20 – 30 cm. Its effect is large – angle scatter of electron which pass through it. Dose uniformity on patient surface will improve particularly on oblique body surfaces. It reduces the depth of penetration and fall off at a shallow depth. Figure 1.11 shows percentage depth dose in humanoid phantom with and without scatter-degrader [22].

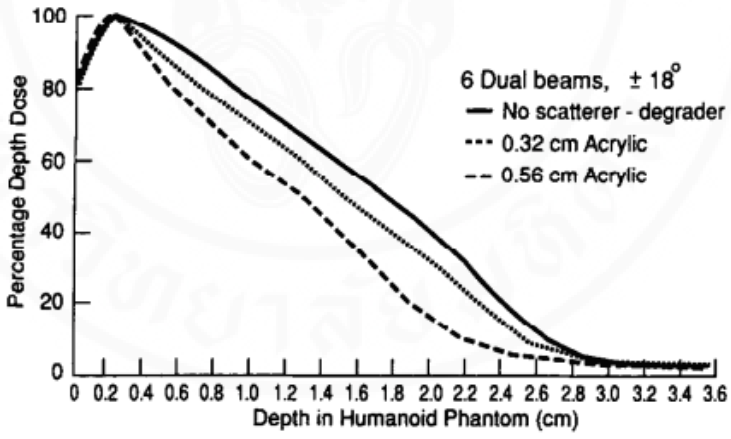

Figure 1.11 The percentage depth doses curve in a humanoid phantom with and without scatterer-degrader.

3.X-ray contamination

X-ray contamination or bremsstrahlung is produced in the exit window of the accelerator, scattering foil, ion chambers, collimators, air, and the patient. The cumulative dose from x-ray contamination over the patient must be known exactly.

A 4 % x-ray dose (~1.5Gy) is unsatisfied in clinical. The x-ray contamination incident on the patient is reduced by angling the beam 10 - 20 degrees above and below the horizontal (Dual angle fields) because the x-rays are predominantly forward-directional. Figure 1.12 shows isodose distribution in y-z plane through the central axis [4]. The x-ray contamination of 0.5 % is peaked in a forward direction along the central axis while off-axis point is the rapid fall off.

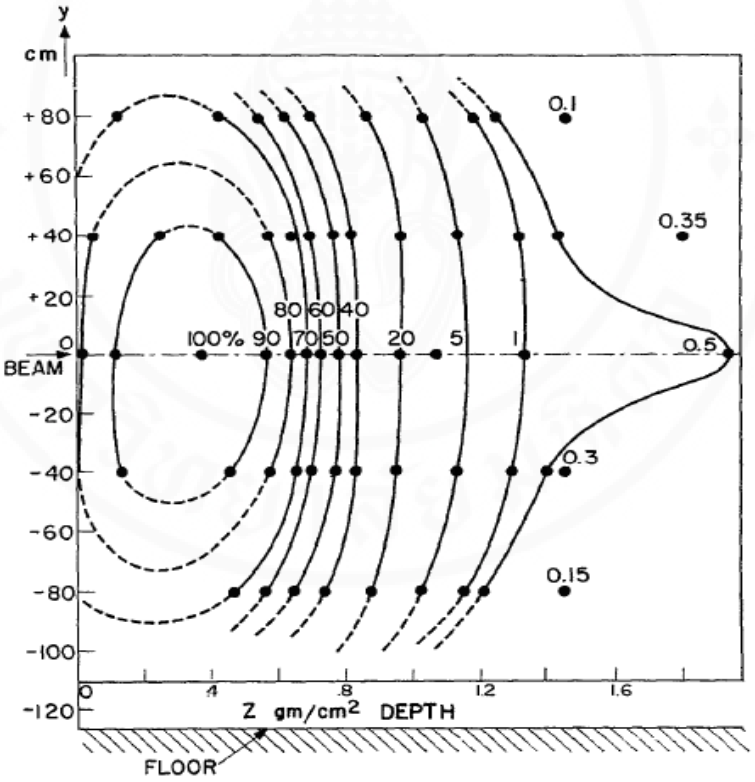

Figure 1.12 Isodose distribution in y-z plane through the central axis for the horizontal beam ($\Theta = 0$)**.**

4. Dose rate and treatment time

Current linear accelerator has a special mode of high dose rate modes at least one electron energy. The dose rate at isocenter is approximately 2500 cGy/min. It can reduce treatment time and also minimize patient motion and fatigue. However, the treatment set-ups are complex cause long set up time in treatment room. The linear accelerators have a heavy workload. One cycle of treatment is divided in two days for Standford technique (six dual field beams), first day AP, RPO and LPO, second day PA, RAO and LAO.

5. Dosimetry

Dosimetry for TSEI technique is difficult and complex. There is review in AAPM23.

Dosimetry phantoms

Various phantoms are used in dosimetric measurements for each purpose.

1. **Water equivalent slab phantoms** made of solid water, polystyrene or Lucite in slab form which have an electron density close to the tissue. Phantom may be used for low energy electron beam dosimetry (R_{50} < 4 g/cm^2, E_0 < 10 MeV). Depth dose measurement in solid phantom can be converted to depth dose-distribution in water by scaling the depth in the phantom to its water-equivalent depth and ionization value at each depth must be scaled by fluence - scaling factor. The values for depth - scaling factor, fluence - scaling factor and density for each plastic are shown in Table 1 [7].

2. Cylindrical phantom of various diameters and made of solid water, polystyrene or lucite. This phantom is used for stimulate the patient's body.

Table 1.1 Values for the depth-scaling factor (c_{pl}),the fluence-scaling factor (h_{pl}) and density for each plastic phantom.

Plastic phantom	c_{pl}	h_{pl}	ρ_{pl} (g/cm^3)
Solid water (WT1)	0.949	1.011	1.020
Solid water (RMI-457)	0.949	1.008[a]	1.030
Plastic water	0.982	0.998[b]	1.013
Virtual water	0.946	—[c]	1.030
PMMA	0.941	1.009	1.190
Clear polystyrene	0.922	1.026	1.060
White polystyrene[d]	0.922	1.019	1.060
A-150	0.948	—[c]	1.127

[a] Average of the values given in Ref. [95] below 10 MeV.
[b] Average of the values given in Ref. [65] below 10 MeV.
[c] Data not available.

3. Anthropomorphic phantom is known as Alderson Rando Phantom, which simulates various body tissues of human such as bone, muscle , lung, and air cavities. The phantom is made of tissue-equivalent material follows ICRU 44 [23] standard. The phantom is shaped into a human torso and section into transversal slices. Each slice has holes which are plugged with pins of soft tissue- equivalent, bone –equivalent or lung equivalent. It has a TLD holder pin that can be inserted into the hole for measurement of dose distribution in various organ. Figure 1.13 shows Anthropomorphic phantom and hole on phantom slice.

Figure 1.13 Anthropomorphic phantom**.**

Detectors

Various detectors are used in dosimetric measurements for each purpose such as parallel-plate ionization chambers, thermoluminescent dosimeters, diode detector, radiographic films and radiochromic films. Their applications and properties are described in section 1.1.5.

Dosimetric measurement

The dosimetry measurement of TSEI is reviewed in AAPM (1987). It is difficult and complex because of absorbed dose measurement at shallow depths with a large area at patient treatment plane. The dosimetry measurements are concluded below.

1. Beam flatness measurement

The electron beam is scattered and spread out in the air before reach the treatment plane. Stationary large field size (36 cm x 36 cm) is insufficient patient dose uniformity for treatment distance of 3-4 m. The used of dual angle field can improve dose uniformity over the patient. A method of determined dual field angle can be used by measurement of relative beam profiles along vertical plane and horizontal plane at treatment plane with variation of dual angle degree from 15 degree to 20 degree. This measurement can be used by film, TLD and diodes. The selection of proper dual angle field is followed AAPM23 that the vertical uniformity of ± 8% and a horizontal uniformity of ± 4 % over 160 cm x 60 cm of treatment plane area. Figure 1.14 shows vertical and transverse beam profiles from a dual angle field (±12º) measured by film [1].

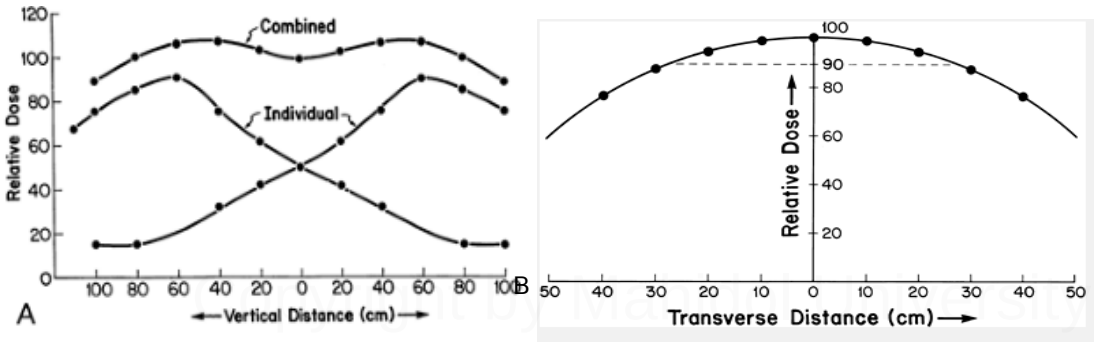

Figure 1.14 Vertical and transversal beam profiles from dual angle field ((±12º)**.**

2. Percentage depth dose measurement

Depth dose distribution along the horizontal axis of the single dual field is measured for determination of depth of maximum dose (D_{max}), beam quality (R_{50}), practical range (R_p) and x-ray contamination. The beam quality and practical range are used to determination of electron beam energy at treatment plane. The percentage depth dose is obtained by parallel plate chamber embedded in solid water phantom and increase depth by increase thickness of slab phantom. It can also be measured by a film sandwiched between a solid water phantom and placed parallel to the horizontal axis. The composite depth-dose distribution for the one complete treatment cycle (six dual fields) may be determined by film sandwiched in the anthropomorphic phantom slab. Depth of maximum dose (D_{max}) and x-ray contamination are also determined from composited depth dose curve. Figure 1.15 shows the percentage depth dose from one complete treatment cycle comparison between single field a in water of electron energy 4 MeV.

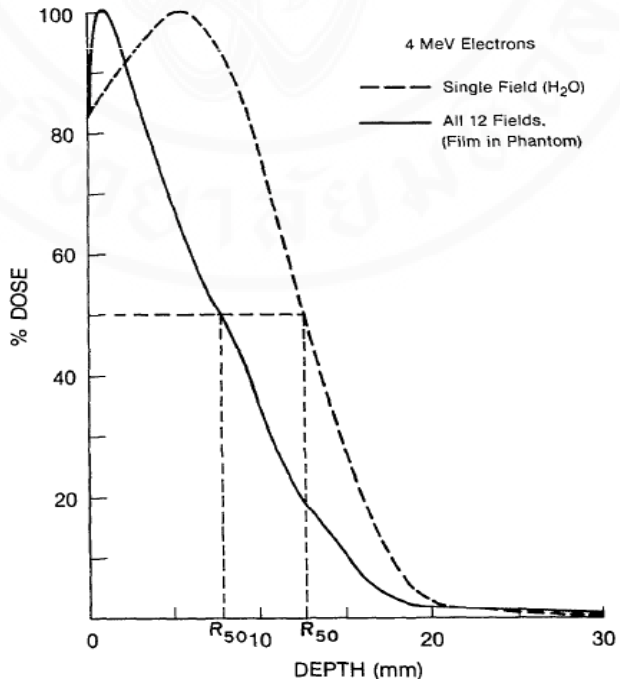

Figure 1.15 The percentage depth dose from one complete treatment cycle comparison between single field in water of electron energy 4 MeV.

3. Calibration point dose measurement

It is an output or absolute dose rate (Gy/MU) at calibration point locates at $(0, 0, d_{max})$ in treatment plan. It is obtained by parallel plate chamber embedded in solid water phantom perpendicular to the horizontal axis at d_{max} (received from percentage depth dose) and irradiate with the single dual field.

4. Treatment skin dose measurement

The treatment skin dose is the mean dose along a circle at or near the surface of a cylindrical polystyrene phantom 30 cm in diameter and 30 cm high that has been irradiated one complete treatment cycle (four, six or eight dual fields). Each field of treatment has been overlap between field so it should have one factor to relate overlapping field. Overlapping factor (B) is the factor that relates the treatment skin dose from one complete treatment cycle to calibration point dose from the single dual beam as an equation.

$$\text{Overlaping factor(B)} = \frac{\text{Treatment skin dose}}{\text{Calibration point dose}} \tag{7}$$

Typically, factor B is range between 2.5 to 3.1 [4].

5. In vivo dosimetry

It is important in TSEI technique for two purposes, the first is determination of dose distribution or uniformity of the patient surface and second is verification of prescribed dose to the patient surface. Thermoluminescent dosimeters (TLD) are most often used for in vivo dosimetry. The TLD must be thin (<0.5 mm) to minimize the effect of dose gradient across the dosimeters. TLD chips are suitable for measurement. It has recommended the calibration of TLD in electron beam energy. Currently, the film has been used for in vivo dosimetry due to the incoming of radiochromic film (self - developing film) that can be cut in small pieces and handle in room light. There are many studies of radiochromic film for in vivo measurement.

CHAPTER II
OBJECTIVE

The objectives of this study is to verify dosimetric parameter that meet the requirements for this TSEI technique using a 6 MeV High Dose Rate Total skin electron Mode (HDTse $^{-}$) of Clinac IX Varian linear accelerator at Ramathibodi hospital.

CHAPTER III
LITERATURE REVIEWS

This research had emphasis on the physical characteristics of Modified Stanford technique. The literatures involved the commissioning of the technique and the dose uniformity on the patient.

Vera Page et al. [14] studied dosimetry measurements under patient treatment conditions in a modification of the Stanford technique or a six field technique that had been replaced the original four field technique in order to receive better uniformity. The study described patient positioning for six-field technique with dual angle field and incorporated two treatment cycles. In order to find optimal conditions for treatment, the dosimetry in a single dual field was measured by measuring the calibration factor using planar ionization chamber and percentage depth dose for different klystron power supply voltages and angular settings. The dose distribution was measured in the treatment plane for determining acceptable vertical uniformity. Moreover, the dosimetry measurements in phantoms was studied for a multiple field treatment using film and TLD by comparing between four-field technique and six field technique in two phantoms ; Circular phantom 27 cm diameter and an Alderson -Rando phantom in order to assess skin dose uniformity and penetration depth for different klystron power supply voltages and angular settings.
Their studies found that calibration factor and penetration increased with increasing klystron power supply voltage and decreasing the angular setting. There studied concluded that single 15° dual fields at a klystron power 11.5 kV was fulfill for the objective of the treatment because it had a good vertical uniformity ,dose variation in treatment plane within ± 5% , the maximum dose at 5 mm depth , 50 percent dose at 1 cm depth , x-ray contamination dropped to 1 % at 2 cm depth . In phantom measurements, it was found that the different klystron power supply voltages and angular settings did not give significant effect on skin dose uniformity. The significant effect was using the multiple field technique. There was better skin dose uniformity in

six-field technique than that in four field technique. The skin dose uniformity was improved from ± 30 % to ±10%. Penetration results were found that they increased with increasing klystron power supply voltages and decreasing the angular settings. Their studies concluded that the changing from four field technique to six field technique had an optimal condition for treatment. Skin dose uniformity was a significant improvement using six field technique. The result of these studies supported the adaptation from four field technique to six field technique or Modified Stanford technique. They suggested to have periodic check calibration point and depth dose for a single dual field if the linear accelerator had been used for many years.

Fraass et al. [24] compared the in- air dose distribution and the actual skin dose distribution on the patients treated with 4 MeV electrons of Modified Stanford technique. The TLD-100 chips were used to determine the dose on different parts. For the in air measurement, TLDs were taped in a small phantom at a position of the patient while for the actual skin measurement, they were taped on the patients' surface. The results showed that the in-air dose distribution had a uniformity while the skin dose distribution was not. The dose different on the trunks was uniform. Several areas were underdose by 20%-30% such as hands, arms, axillas and forehead. They concluded that the in-air distribution measurement was not sufficient in a measurement of the dose uniformity. The patient dose distribution should be measured to determine the local treatment technique, the certain low dose region and the shielding region during treatment.

Yavus et al. [25] studied skin dose uniformity of mycosis fungoides patients' treatment between 1994 and 2000 with Stanford technique. Thermoluminescence measurement was made at 10 points of patients, such as vertex, umbilicus, sternum, back and top of shoulders, elbows, palms, lateral abdominal wall, knees, and dorsal feet. The mean values of TLDs reading related to TLD reading in prescription point (umbilicus) were used to study dose uniformity throughout the skin surface. Moreover they evaluated intra-patient dosimetric variation between 2 fractions and the effect of degrader thickness on dose uniformity. They found that dose uniformity throughout the skin surface was 15% compared with ± 5% dose uniformity on humanoid phantom 's surface. The uniformity at trunk was better than extra-trunk which was the mobile parts of the body. The skin dose uniformity of thick degrader

was worse than the thin degrader. There was minimal improvement of dose uniformity in the next treatment. They suggested that TLD was a useful detector for in vivo measurement and routine in treatment.

Indra J. Das et al. [26] studied the spatial distribution of the bremsstrahlung dose profile along the entire length of patient phantom 2 m tall from dual angle beam technique (± 17° gantry angle) in TSEI. This study compared between thermoluminescent measurement and ionization chamber measurement at depth 4 cm along a patient's plane. In ionization measurement, it was shown that the large different magnitude and dose distribution profile was between +17° and -17° gantry angle. The peak magnitude in + 17° gantry angle was 2.5 times greater than the peak magnitude in - 17° gantry angle and asymmetry total bremsstrahlung dose profile when two dose distribution were added together. This result was due to a cable effect. The ionization chamber cable responded in a large electron field caused radiation induce current when gantry angle projected to the floor (- 17°). In thermoluminescent measurement, it was shown that the same magnitude and a dose distribution profile were between +17° and -17° gantry angle and symmetry total bremsstrahlung dose profile. The absolute bremsstrahlung dose was approximately 1% of electron dose. The bremsstrahlung peak distance was 1.3 m. They suggested that bremmstrahlung dose measurement should be done in patient geometry and treatment technique for each user's machine and be preferred of using a cable – free detector (film, TLD, Fricke) in a measurement bremsstrahlung dose in the large electron field.

El –Khatib et al. [22] studied the effect of beam uniformity on different scatterer-degraders and beam angulations. They measured vertical beam profiles with plane parallel chamber at 1 cm depth in polystyrene phantom at gantry angle ± 14°, ± 16°, ± 18°, ± 20° and ± 22° with no beam scatterer to determine dual angle which made optimal uniform dose profile within ± 8% over 160 cm of treatment plane (AAPM 23). The optimal gantry angle was ± 18°. However, when acrylic scatterer 0.32 cm thickness was mouthed on gantry head , they found that gantry angle ± 18° didn't have optimal uniform dose profile but there was good uniformity in gantry angle ± 21°. They measured percentage depth dose (PDD) on dual beam without beam scatterer , with acrylic scatterer 0.32 cm and 0.56 cm thickness mouthed on gantry head . The results showed that acrylic scatterer 0.32 cm thickness produced the

required penetration (R_{80} ~ 7 – 8 mm, R_{50} ~ 14-15 mm). Their studies concluded that different beam penetration can be obtained by using different thicknesses of scatterer – degrader from the same high dose rate mode energy of 6 MeV on linear accelerator. The new beam angulation must be determined for optimal vertical beam uniformity.

CHAPTER IV
MATERIALS AND METHODS

4.1 Materials

4.1.1 Linear accelerator

Clinac iX (Varian Radiation Oncology System, Palo Alto, CA) linear accelerator with a Millenium^{TM}120 leaf MLC at Ramathibodi hospital shown in Figure 4.1 was used in this experiment. This machine can produce two photon beam energies with 6 and 10 MV, six electron beam energies of 4, 6, 9, 12, 16 and 20 MeV. Photon beam field sizes at isocenter are range from 0.5 × 0.5 cm^2 to 40×40 cm^2. Electron beam field sizes are collimated by applicator cones sizes from 6 × 6 cm^2 to 25 × 25 cm^2. The MV Electronic portal imaging device (EPID) mounted on a retractable arm attached to the gantry is used for patient setup verification. It has a special treatment mode called Total Body Irradiation (TBI) which use the photon beam treatment (6 MV in Ramathibodi) and a 6 MeV High Dose Rate Total skin electron Mode (HDTse $^{-}$) for TSEI treatment.

High Dose Rate Total skin electron Mode (HDTse $^{-}$) is a special treatment mode delivering electron beam (nominal energy of 6 or 9 MeV) at high dose rate for total skin electron irradiation. The dose rate at 1.6 m is 888 MU/min, approximately 2500 cGy/min at the isocenter. A special accessory tray called MLC HDTSe^{-} 6MeV is inserted into the wedge slot on the head of the gantry (Figure 4.2), the collimators setting is opened automatically 36 x 36 cm^2 at the isocenter. There is no requirement for additional electron applicators. A password is set for this special technique in order to prevent unauthorized person used in this mode.

Figure 4.1 Medical linear accelerator Varian Clinac iX.

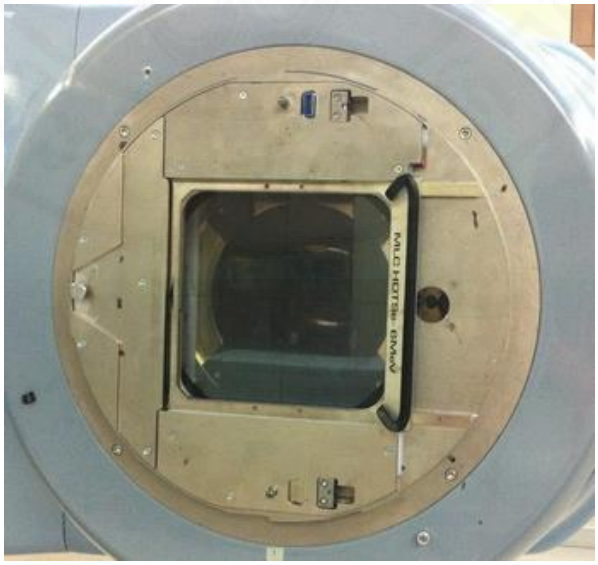

Figure 4.2 MLC HDTSe- 6MeV accessory tray is inserted into the wedge slot on the head of the gantry.

4.1.2 Patient positioning device and scatterer - degrader

A wooden stand shown in Figure 4.3 is constructed for positioning and supporting patient during TSEI treatment. Its dimensions of 210 cm in height and 105 cm in width with platform 100 × 100 cm^2 mounted on the wheel with brakes for portability. The platform can be elevated from 25 cm to 60 cm (5 cm for each step) above floor level. It has four hand grips and a backrest that can be adjusted to the optimal position to support the patient. Scatterer - degrader shown in Figure 4.3 made of 0.5 cm thick perspex sheet with the dimension of 200 cm × 100 cm elevated 25 cm above floor. These thickness selection accounts for the penetration depth which adequate to the depth of lesion [2].

(a). (b).

Figure 4.3 (a).Patient positioning device and (b) Scatter – degrader.

4.1.3 Plane – parallel ionization chamber and Dose 1 electrometer

The Roos chamber type -34001 (PTW, Freiburg, Germany) shown Figure 4.4 was used in the experiment. Its sensitive volume is 0.35 cm^3 which thin PMMA entrance window thickness 1 mm. The inner radius of the measuring volume is 12 mm and collecting electrode diameter is 15.6 mm. The reference point for measurement is set on 1 mm below entrance window.

Dose 1 electrometer was used with ionization chambers for absorbed dose measurement. It has two measuring mode, charge (Coulomb) and current (Ampere). Bias voltage for Roos chamber is ± 300 V.

Figure 4.4 Parallel plate Roos chamber and Dose 1 electrometer.

4.1.4 Thermolunescent dosimeter (TLD)

TLD-100 chip used in this measurement was Lithium fluoride doped with magnesium and titanium (LiF:Mg,Ti). It consists of ^{7} Li 92.5% and ^{6} Li 7.5% . An effective atomic number is 8.2 which is nearly equivalent to 7.4 of tissue. It is well suited for in vivo measurement. TLD chip size is $3 \times 3 \times 0.15$ mm^3.

The irradiated TLD signal was read by the automatic TLD reader system Harshaw 5500 [27] shown in Figure 4.5. Automatic reading 50 dosimeters. Heating procedure was hot nitrogen gas, which a linear ramp temperature up to 400 °C. The TLD was calibrated with a Roos chamber in 6 MeV electron beam.

Figure 4.5 TLD- 100 chip and TLD reader system Harshaw 5500.

4.1.5 An anthropomorphic phantom (Alderson Rando phantom)

An anthropomorphic phantom illustrated in Figure 4.6 is modeled of tissue equivalent material with 0.985 g/cm^3 density and 7.3 effective atomic number. It was designed by following ICRU-44 standards. The phantom's size is 155 cm tall and weighs 50 kg. It has transverse slice with 2.5 cm thickness. Each slice contains holes with the separation between holes of 1.5 cm. Holes can be plugged with pins of lung tissue equivalent, soft-tissue-equivalent, bone-equivalent and TLD holder pins.

Figure 4.6 An anthropomorphic phantom.

4.1.6 Solid water phantom

Figure 4.7 shows the solid water phantom material (Gammex RMI). It was made of epoxy resins and powder control density and a radiation property. It has 1.030 g/cm^3 density and 5.96 effective atomic numbers. Its physical form is a square slab of 30 x30 cm^2 with various thickness of 0.2 , 0.5, 1, 2, and 5 cm.

Figure 4.7 Solid water phantom (Gammex RMI).

4.1.7 Cylindrical phantom

Figure 4.8 shows Cylindrical White Poly Ethylene Phantom 30 cm in height and 26 cm in diameter is used in this measurement. It is covered around by bolus 2 cm thickness in order to meet the definition of phantom in treatment skin dose measurement (30 cm in height and 30 cm in diameter).

Figure 4.8 Cylindrical phantom.

4.1.8 Radiochromic film (GAFCHROMIC ® EBT2 Film)

GAFCHROMIC ® EBT2 Film (International Specialty Products Inc., Wayne, NJ) is a self-developing film for radiotherapy dosimetry. The EBT2 film was a waterproof film, high spatial resolution (< 0.1 mm), near tissue equivalent (Z_{eff} = 6.84 compared to Z^{water}_{eff} = 7.3), low energy dependence. EBT2 was made by combining a clear, polyester with the action film (radiation sensitive component) coating, over with a topcoat. The clear polyester over-laminate with the adhesive layer bounded to the coated side of active layer in order to protect the active layer/topcoat from mechanical damage such as water. The film responds to radiation exposure by forming a blue colored polymer with an absorption peak at 636 nm. EBT2 film has a dose range of 0.01 – 8 Gy. In this measurement, EBT2 film was used for percentage depth dose measurement and the dose distribution in the treatment plane.

Figure 4.9 GAFCHROMIC ® EBT2 Film.

4.1.9 Film digitizer and ImageJ program software

VIDAR's DosimetryPRO® Advantage(Red) (Vidar Systems Corporation, Herndon, VA, USA) is CCD scanner used for film dosimetry. This scanner uses a long, diffuse light source to illuminate film and image on film is projected on 2-dimension CCD array. It has red LED light source with maximum emission of 627 nm that closely matched to the absorption peak of EBT2 film at 636 nm. Its function consists of color depth of 8 bit, 12 bit and 16 bit grayscale and spatial resolution varies from 71 dpi to 150 dpi. In this measurement, an exposed film was scanned with 16 bit grayscale and spatial resolution of 71 dpi. ImageJ (National Institute of Mental Health, Bethesda, Maryland, USA) is a public domain Java image processing. It can display, edit, analyze, process, save and print of 8- bit, 16- bit and 32-bit images. It can read many image formats such as TIFF, GIF, JPEG, BMP, DICOM, FITS or “raw” formats.

Figure 4.10 VIDAR's DosimetryPRO® Advantage(Red).

4.2 Methods

4.2.1 Selection of technique and design for proper positioning device followed by AAPM Report 23

Modified Stanford technique or Six-dual angle field technique has been selected to used in this research due to identical size of the treatment room and uncomplicated positioning device management. This technique was most commonly used in many institutes. It had the optimal dosimetry results to meet the requirements for TSEI treatment that has been reviewed in many literatures.

Figure 4.11 shows the physical characteristics of Modified Stanford technique in Ramathibodi hospital. The patient is standing on a wooden treatment stand with long SSD 380 cm (accounting for the size of treatment room). A large 0.5 cm width Scatterer degrader (perspex sheet) is placed in front of treatment plane 30 cm that receive from the vertical uniformity measurement.

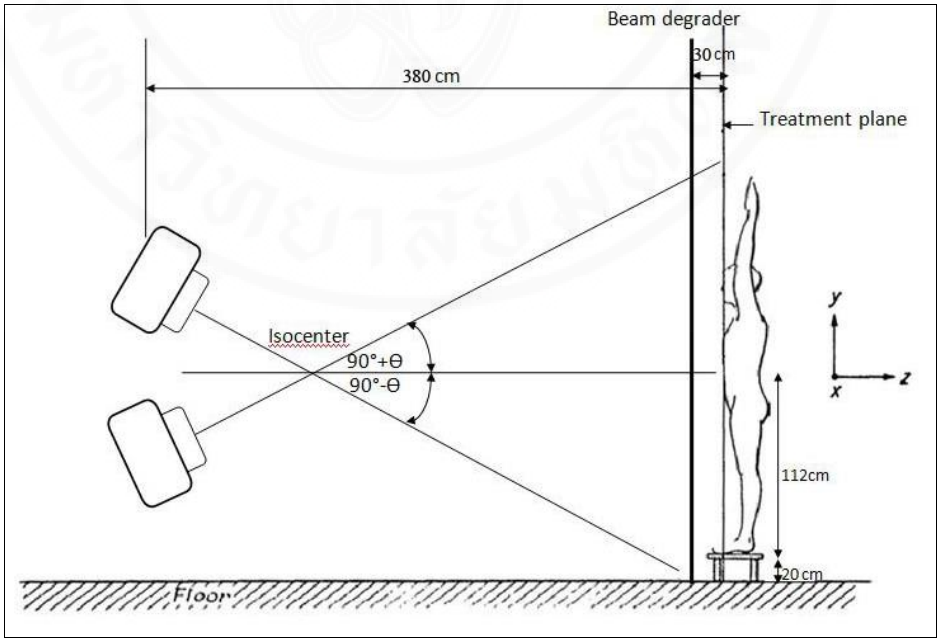

Figure 4.11 Treatment geometry setting of Modified Stanford technique.

4.2.2 Optimization of treatment geometry and dosimetry data

Geometry set up for dosimetry measurement were divided into:

a) Dual angle fields beam: Gantry was angled above and below the horizontal beam. These set up provides the dosimetry data in planar plane at the treatment plane.

b) Six dual angle field beam: Sum of six dual field beam with 60º separation on phantom orientation. These set up provides the dosimetry data in complete treatment.

4.2.3.1 Dual angle field beam

The gantry was angling above and below the horizontal beam SSD 380 cm from treatment plane, scatterer –degrader thickness of 0.5 cm was placed in front of treatment plane. This geometry setup was prepared to find the followings:

a) Optimal tilt angle

To find tilt angles that have optimal dose uniformity in vertical plane and horizontal plane at treatment plane following AAPM 23 [4].

The Roos chamber was placed on solid water phantom which its center perpendicular to beam direction. It was moved in vertical direction every 20 cm step from the center (-80 cm to 80 cm). The high dose rate mode 6 MeV electron beam was irradiated with gantry angle ± 17º, 500 MU/angle. The ionization value was measured by Dose 1 electrometer at voltage +100V then relative dose profile along vertical axis normalize to center of the beam was plotted. The measurement was repeated for gantry angle step 0.5 º until ± 20 º. The same gantry angle was used in dose profile measurement along horizontal axis which chamber was moved in horizontal direction every 10 cm step from center (-40 cm to 40 cm). The Relative dose curves of all tilt angles were plotting together in order to compare the optimal tilt angle provided by AAPM 23 which stated that the optimal dose distribution in vertical plane and horizontal plane shoud be ± 8% and ± 4% respectively.

b) Optimal distance of scatterer - degrader

This measurement compared the effect of variation distance of scatterer - degrader from the treatment plane in order to receive optimal dose uniformity from

optimal distance.The chamber was placed on solid water phantom which its center perpendicular to beam direction. The scatterer – degrader was placed in front of treatment plane 30 cm. The chamber was moved in vertical direction every 20 cm step. The high dose rate mode 6 MeV electron beam was irradiated with optimal tilt angle (obtained from a).) 500 MU/angle. The ionization value was measured by Dose 1 at voltage +100V then plot relative dose profile along vertical axis normalize to the center of the beam. The measurement was repeated for scatterer – degrader distance 40 and 50 cm. The Relative dose profiles of each scatterer – degrader distance were plotting together.

c) 2D dose distribution

TLD chips were placed on wood in grid point size 10 x 10 cm^2 shown in Figure 4.12. The 6 MeV high dose rate mode electron beam was irradiated with optimal tilt angle (obtained from a).). TLD chips were read by the automatic TLD reader, then doses were calculated in a relative dose related to dose at the center of the beam. Mean relative dose (± %) was calculated in area 180 x 60 cm^2.

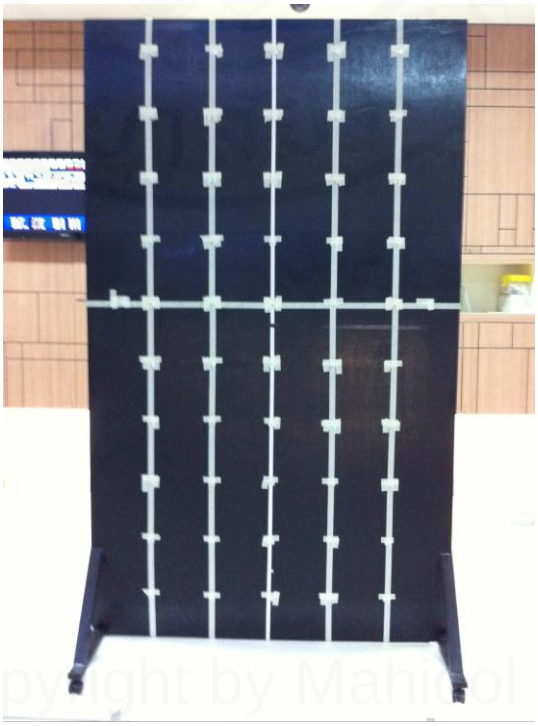

Figure 4.12 TLD chip placement for 2D dose distribution measurement.

d) Percentage depth dose measurement

To determined beam quality (R_{50}) , practical range (R_p) by parallel plate Roos chamber compared with EBT2 film.

Percentage depth dose measured by parallel plate chamber

The chamber was placed on solid water phantom which its center perpendicular to the beam direction. The 6 MeV high dose rate mode electron beam was irradiated with optimal tilt angle (obtained from a).) 500 MU/angle. The ionization value was measured by Dose 1 at voltage +100V. Solid water phantom slab was increased 2 mm step until 30 mm.

Percentage depth ionization curve (PDI) was created from ionization value in any depth (I_d) relative to ionization value at depth of maximum dose (I_{max}) from equation (8).

$$PDI = \frac{I_d}{I_{\max}} x100 \qquad (8)$$

Percentage depth ionization curve (PDI) was converted to percentage depth dose in water (PDD) by scaling each measurement depth in phantom (z_{pl}) from equation

$$z_w = z_{pl} c_{pl} \quad \text{g/cm}^2 \qquad (9)$$

Ionization value was scaled from equation

$$M_Q = M_{Q,pl} h_{pl} \qquad (10)$$

Where h_{pl} is the fluence-scaling factor for certain plastic (=1.008 for RMI)

and multiplying stopping- power ratio $S_{w,air}$ at each depth according to TRS 398.

The beam quanlity (R_{50}) is the half- value of depth dose distribution in water was obtained from the percentage depth ionization curve (PDI).

The half - value of depth-ionization in phantom ($R_{50,ion,pl}$) was converted to $R_{50,ion}$ from equation :

$$R_{50,ion} = R_{50,ion,pl} c_{pl} \quad \text{g/cm}^2 \qquad (11)$$

Where $R_{50,ion,pl}$ is the half- value of the depth –ionization distribution in plastic

c_{pl} is the depth-scaling factor (= 0.949 for RMI 547)

The half value of depth dose distribution in water R_{50} was obtained from equation :

$$R_{50} = 1.029R_{50,ion} - 0.06 \ \text{g/cm}^2 \quad (\text{for } R_{50,ion} \leq 10 \ \text{g/cm}^2) \tag{12}$$

Mean energy at phantom surface (treatment plane) was obtained by

$$\bar{E}_0[\text{MeV}] = 2.33R_{50} \tag{13}$$

Determine practical range (R_p) and x-ray contamination from the curve in order to calculate the most probable energy at phantom surface from the equation (14).

$$E_{p,o}[MeV] = 0.22 + 1.98R_p + 0.0025R_p^2 \tag{14}$$

Figure 4.13 Percentage depth dose measurement using Roos chamber.

In order to study the effect of scatter degrader, the percentage depth dose curve was measured without degrader also.

Percentage depth dose measured by EBT2 film

The 8 x 10 inch^2 film was placed between a slab of solid water phantom. The margin of the film was parallel to the margin of solid water phantom and the center of the beam. The 6 MeV high dose rate mode electron beam was irradiated with optimal tilt angle (obtained from a). 500 MU / angle. After 24 h irradiation, films were scanned by Vidar scanner. The film images were saved in TIFF format and analyzed by ImageJ software. The pixel value from image were converted to dose by calibration curve that was made previously. The percentage depth dose curve was created from those in any depth (D_d) relative to a maximum dose $(D_{\max})$ from the equation (15).

$$PDD = \frac{D_d}{D_{\max}} x100 \qquad (15)$$

The beam quality (R_{50}) , practical range (R_p) were obtained from percentage depth dose curve. The mean energy at the phantom surface ($\bar{E}_0$) and most probable energy ($E_{p,0}$) were also obtained by equation (13) and (14) respectively.

Percentage depth dose curve from chamber measurement was compared with a percentage depth dose curve from EBT2 film measurement.

e) Calibration point dose measurement

The calibration point dose is output or absolute dose rate (cGy / MU) at $(0, 0, d_{max})$ in treatment plane at SSD = 380 cm.

This measurement showed the comparison of calibration point dose between two measurement protocols. The First protocol was IAEA TRS 398 which measured dose at reference depth (z_{ref}) and converted to dose at a depth of maximum dose (z_{max}) by percentage depth dose .The second protocol was AAPM report 23 which measured dose at a depth of maximum dose (z_{max}).

1) Measurement of calibration point dose following IAEA protocol TRS 398

The Roos chamber was placed on solid water phantom shown in Figure 4.14 at reference depth $z_{ref,pl}$ following IAEA protocol TRS 398. The center was perpendicular to the beam direction. The reference depth in water was calculated from equation (16).

$$z_{ref} = 0.6R_{50} - 0.1 \quad g/cm^2 \tag{16}$$

The conversion of the reference depth in water z_{ref} to reference depth in plastic $z_{ref,pl}$ by using equation :

$$z_{ref,pl} = z_{ref} / c_{pl} \quad g/cm^2 \tag{17}$$

Where c_{pl} is the depth-scaling factor (= 0.949 for RMI 547)

The 6 MeV electron beam was irradiated with optimal tilt angle (received from a) measured by electrometer, The measurements were performed at +300 V, -300 V and 100 V for correcting of the recombination (k_s) and polarity effects (k_{pol}).

The ionization value at depth $z_{ref,pl}$ in phantom ($M_{Q,pl}$) was scaled to an ionization value at z_{ref} in the water (M_Q) by

$$M_Q = M_{Q,pl} h_{pl} \quad (18)$$

Where h_{pl} is the fluence-scaling factor for certain plastic (=1.008for RMI)

Absorbed dose was calculated following IAEA protocol TRS 398 from equation

$$D_{w,Q} = M_Q k_s k_{pol} k_{TP} k_{elec} N_{D,W,Q_0} k_Q \quad \text{cGy MU}^{-1} \quad (19)$$

Where M_Q is the reading corrected for the influence factor

N_{D,w,Q_0} is the absorbed dose to water calibration factor for PTW Roos chamber that has been calibrated in electron beam from Secondary Standard Dosimetry Laboratory (SSDL), The factor was obtained by interpolation from beam quality (R_{50}).

k_Q = 1, due to the chamber has been calibrated in electron beam

The absolute dose rate at z_{ref} was converted to that at z_{max} through PDD value by

$$D_{w,Q}(z_{max}) = \frac{D_{w,Q}(z_{ref})}{PDD(z_{ref})} x100 \quad \text{cGy MU}^{-1} \quad (20)$$

2) Measurement of calibration point dose following AAPM report 23

The Roos chamber was placed on solid water phantom at a depth of maximum dose (z_{max}). Depth of maximum dose received from percentage depth dose measurement (c). The 6 MeV electron beam was irradiated with optimal tilt angle (obtained from a).The measurements were performed at +300 V, -300 V and 100 V for calculating the recombination correction (k_s) and polarity correction (k_{pol}). The absolute dose rate was obtained from equation (19).

The calibration point dose from two measurements were compared.

Figure 4.14 Calibration point dose measurement

4.2.3.2 Six dual angle field beam

The gantry was angling above and below the horizontal beam SSD 380 cm from treatment plane , the optimal distance of scatterer – degrader was placed at 30 cm in front of the treatment plane. Six phantom positions were arranged relative to each of the dual angle beams. This geometry was setup to find the followings:

a) Treatment skin dose measurement

Treatment skin dose is a mean dose along a circle at or near the surface of cylindrical polystyrene phantom 30 cm in diameter and 30 cm high which has been irradiated with six dual fields (AAPM 23).

Cylindrical phantom 30 cm in high and 26 cm in diameter was covered around by bolus 2 cm thickness as shown in Figure 4.15 in order to meet the definition of phantom by AAPM 23 recommendation. TLD chips were placed on the surface of phantom at 30° intervals. The 6 MeV electron beam was irradiated with optimal tilt angle for 60° phantom rotation,500 MU / angle. TLD chips were read by the automatic TLD reader then calculated average dose value in the unit of cGy/MU.

Figure 4.15 Treatment skin dose measurement.

b) Overlapping factor (B)

Overlapping factor or factor B is the relation between treatment skin dose (Six dual field) to calibration point dose (Dual field) calculated by equation (21):

$$Overlapping\ \ factor = \frac{Treatment\ skin\ dose}{Calibration\ point\ dose} \tag{21}$$

Where

Treatment skin dose is the average dose on surface of cylindrical phantom from six dual field beam.

Calibration point dose is the absolute dose rate (Gy/MU) at depth ofmaximum dose from dual angle beam

The treatment skin dose should be higher than the calibration point dose 2-3 times.

c) MU calculation

The MU/angle was calculated by equation (22):

$$MU = \frac{\text{Pr}escribe\ dose\ per\ treatment\ cycle}{Output(cGy/MU)xB} \tag{22}$$

Where

Prescribed dose per treatment cycle (cGy) is the dose for one complete cycle from six dual field beam.

Output is the calibration point dose from dual angle beam.

Factor B is overlapping factor received from the relation between treatment skin dose (Six dual field) to calibration point dose (Dual field).

d) Percentage depth dose measurement

Percentage depth dose measurements by film placed in the slab of Rando phantomwhich has been irradiated with six dual fields .

The 8 x 10 inch^2 films were placed between slabs of Rando phantom on skin level , chest level and abdomen (umbilicus level). The films were cut to fit with the shape of each section and placed their rim parallel to the margin of Rando phantom. The 6 MeV electron beam was irradiated with optimal tilt angle (obtained from a).) for one complete treatment cycle, six phantom positions : AP, PA, RAO, LAO, RPO and LPO. The prescribed dose was 200 cGy which the MU/angle was calculated from equation (22)**.** After 24 hour irradiation, films were scanned by Vidar scanner. The film images were saved in TIFF format and analyzed by ImageJ software. The pixel value from image were converted to dose by calibration curve that was made previously. The percentage depth dose curve was created from those in any depth (D_d) relative to a maximum dose (D_{max}) from equation (15). The beam quality (R_{50}) , practical range (R_p) and x – ray contamination were determined from percentage depth dose curve.

Figure 4.16 Treatment geometry set-up on Rando phantom.

e) Dose uniformity on Rando phantom

TLD chips were sealed in plastic bags and taped on surface of phantom at various locations such as umbilicus, chest, vertex, both axillas, abdomen, back and mid of femurs.

The 6 MeV high dose rate mode electron beam was irradiated with optimal tilt angle (obtained from a) for one complete treatment cycle. Six phantom positions : AP PA, RAO, LAO, RPO and LPO are shown in Figure 4.17.

The prescribed dose was 200 cGy which the MU/angle was calculated from equation (22). TLD chips were read by the automatic TLD reader. The doses at various locations were normalized to dose at the umbilicus (prescription point).

Figure 4.17 Six phantom positions for one complete treatment cycle.

CHAPTER V
RESULTS AND DISCUSSIONS

5.1 Optimization of treatment geometry and dosimetry data

5.2.1 Dual angle field beam

a) Optimal tilt angle

Figure 5.1 shows the results of relative dose profile measurements along vertical axis distance (80 cm to -80 cm) for different tilt angle from ± 17º to ± 20º with 0.5 º step. AAPM report 23 [4] recommended that the beam uniformity along superior to inferior (vertical uniformity) is ± 8% and a horizontal uniformity is ± 4 % over 160 cm x 60 cm of treatment plane area. The ± 18º tilt angle shows the best dose vertical uniformity that has percent relative dose ± 8% within 160 cm. The asymmetry of the upper and lower profile was due to increasing by scattering from the floor.

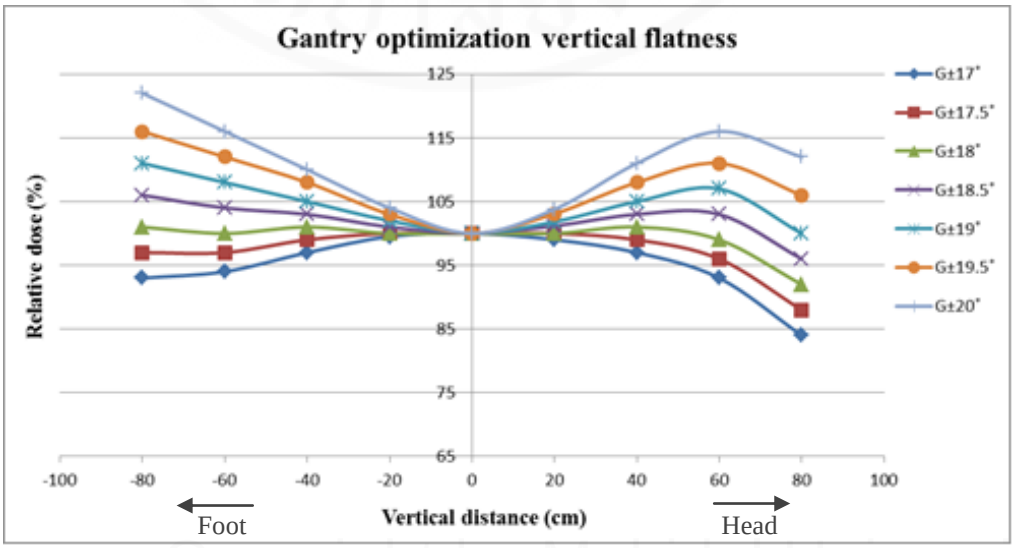

Figure 5.1 Relative dose profile measurement along vertical axis distance for different tilt angles by ionization chamber.

Figure 5.2 shows the relative dose profile measurement along horizontal axis distance from optimal tilt angle ± 18º.

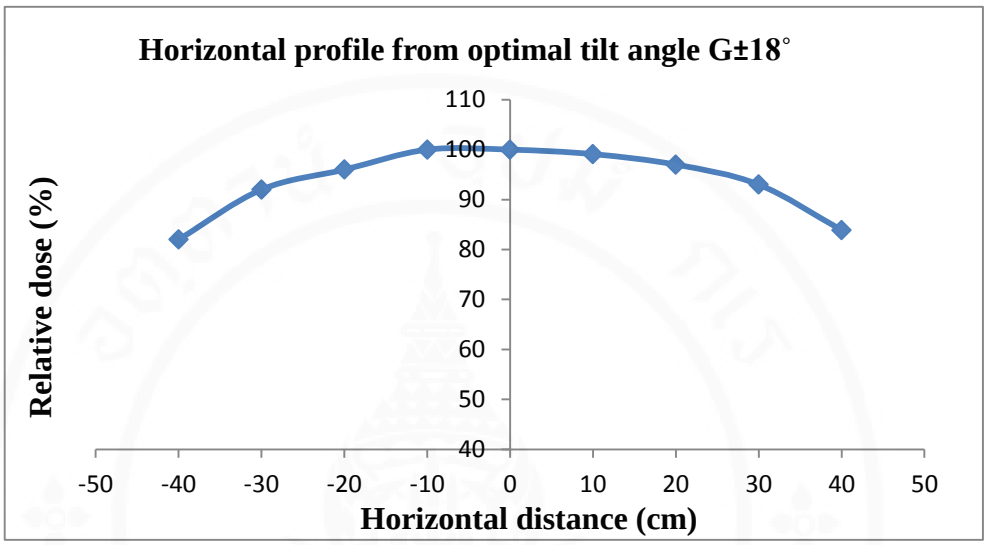

Figure 5.2 Relative dose profile measurement along horizontal axis distance for optimal tilt angle ± 18º.

Figure 5.3 shows the comparison of relative dose profile measurement along horizontal axis distance from optimal tilt angle ± 18º, ±19º and 0º.

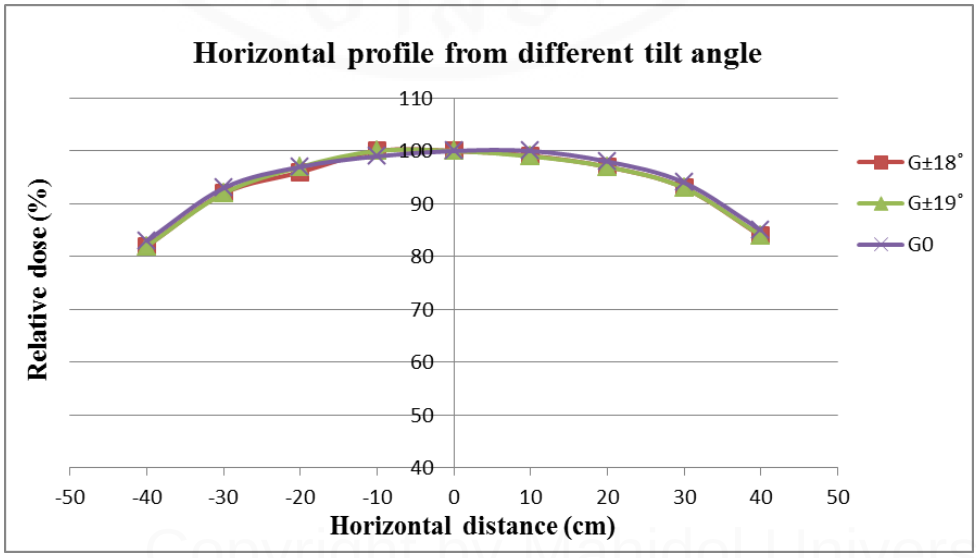

Figure 5.3 Relative dose profile measurement along horizontal axis distance for different tilt angles.

Figure 5.4 shows the comparison of relative dose profile measurement along vertical axis distance from optimal tilt angle ± 18º which scatterer- degrader distance were varied from treatment plane 30,40 and 50 cm. The results showed that dose uniformity were not different on lower profile but a little different on upper profile between distance 30 and 50 cm. Upper profile of scatterer- degrader distance 50 cm was lower than that of degrader distance 30 cm due to lack of scattering to the treatment plane.

Scatterer - degrader distance 30 cm from treatment plane was selected to treatment geometry setup of TSEI technique.

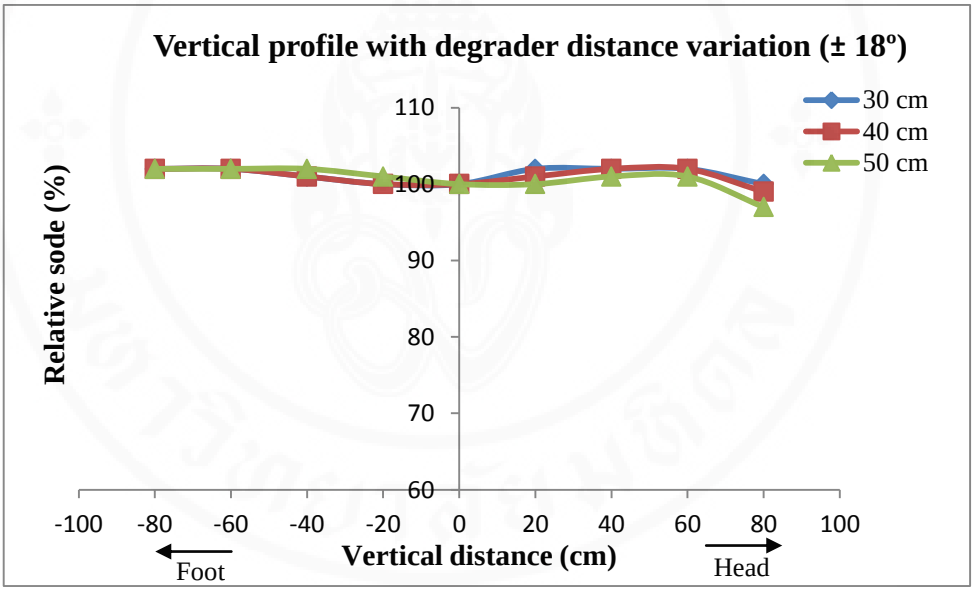

Figure 5.4 Relative dose profile measurement along vertical distance from scatterer - degrader distances among 30, 40 and 50 cm.

b) 2D dose distribution

Figure 5.5 shows the relative dose distribution in area 180 x 80 cm^2 from optimal tilt angle ± 18º with a scatterer - degrader 30 cm distance. Dose values are normalized to 100% at the horizontal axis. The Figure shows that it has a relative dose between 90% – 108 % in area 180 x 80 cm^2. The mean relative dose was 99% ± 4% and 95% ± 6 % for area 180 x 60 cm^2 and area 180 × 80 cm^2 respectively.

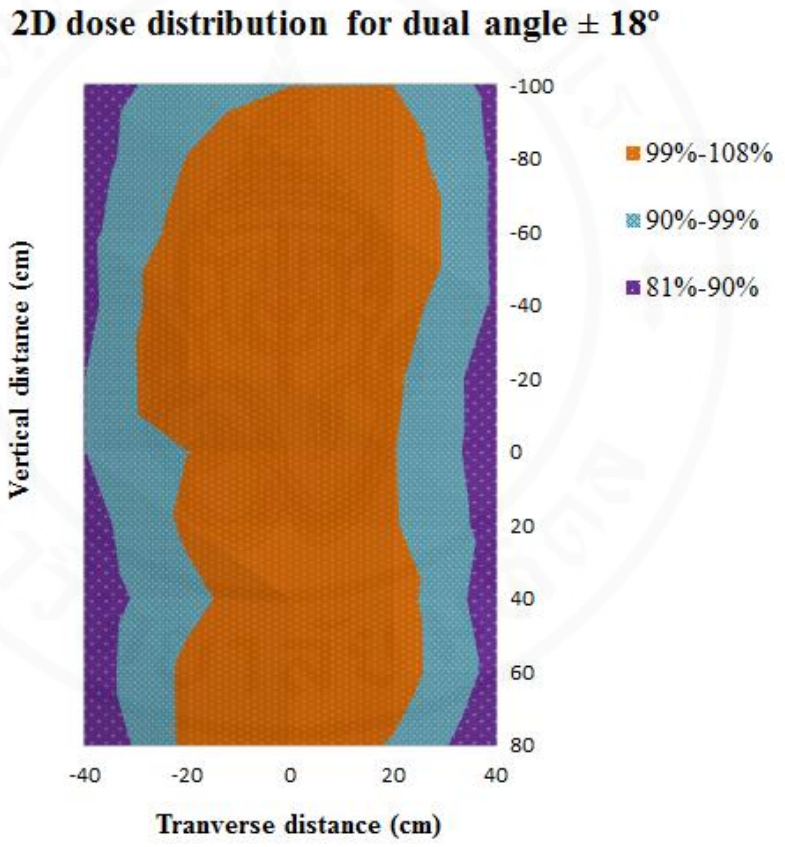

Figure 5.5 2D dose distribution from dual angle ±18º.

c) Percentage depth dose measurement

Percentage depth dose measured by parallel plate chamber

Figure 5.6 shows the percentage depth dose curves using parallel plate Roos chamber in solid water phantom at the treatment plane compared between dual angle beam (gantry 72º,108º) and single horizontal beam (gantry 90º).The two curves are almost superimposed.

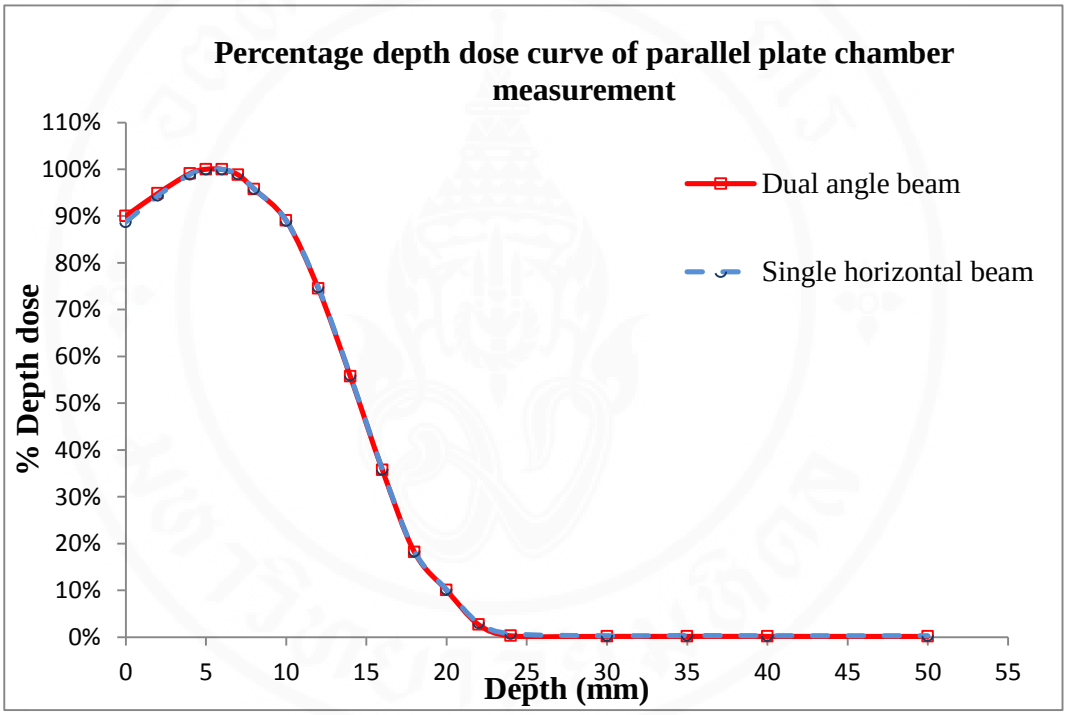

Figure 5.6 Percentage depth dose curve comparison between dual angle beam and single horizontal beam measured by parallel plate chamber.

From the percentage depth dose curve of dual angle beam, it was found that R_{50} =14.3 mm. Tthe mean energy at treatment plane was obtained from (13).

$$\bar{E}_0 = 2.33 \times 1.43$$

$$= 3.3 \text{ MeV}$$

The practical range (R_p) = 19.5 mm and the most probable energy at phantom surface was obtained from the equation (14).

$$E_{p,o}[\text{MeV}] = 0.22 + 1.98(1.95) + 0.0025(1.95)^2$$

$$= 4.1\text{MeV}$$

Percentage depth dose measured by EBT2 film

Figure 5.7 shows the percentage depth dose curves using EBT2 film placed between a slab of solid water phantom at the treatment plane compared between single horizontal beam (gantry 90º) and dual angle beam (gantry 72º,108º). The two curves are almost superimposed which corresponding to result of parallel plate Roos chamber measurement.

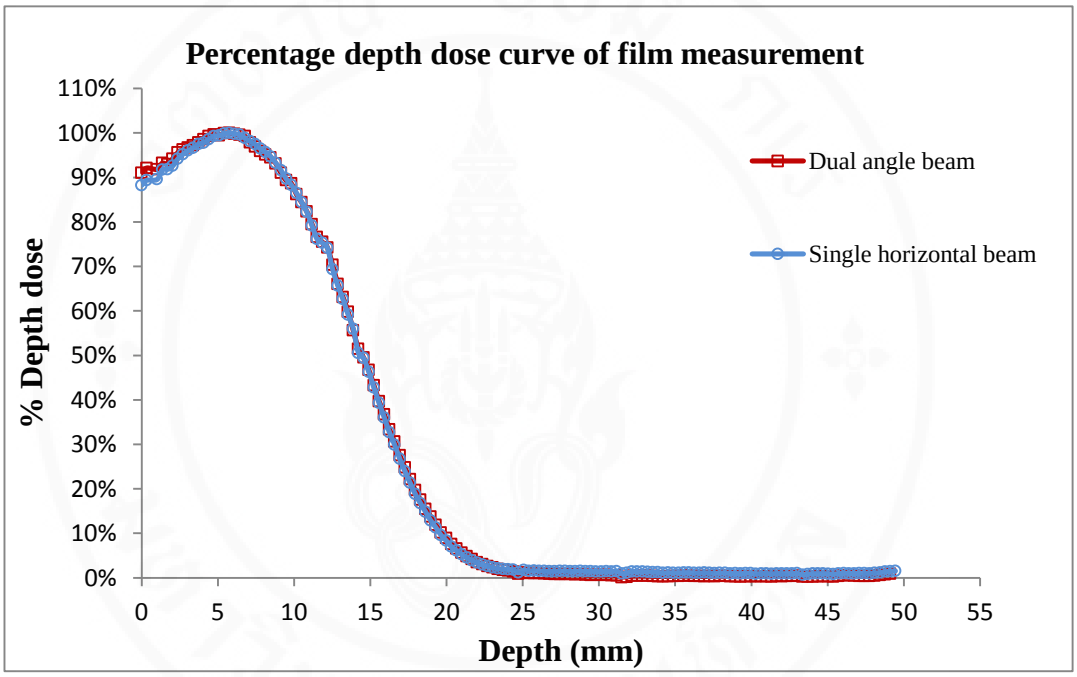

Figure 5.7 Percentages depth dose curve comparison between dual angle beam a single horizontal beam measurement by EBT2 film.

From the percentage depth dose curve of dual angle beam, it was found that R_{50} = 14.5 mm. The mean energy at treatment plane was obtained from (13).

$$\bar{E}_0 = 2.33 \times 1.45$$

$$= 3.4 \text{ MeV}$$

The practical range (R_p) = 20 mm and the most probable energy at phantom surface was obtained from the equation (14).

$$E_{p,o}[\text{MeV}] = 0.22 + 1.98(20) + 0.0025(20)^2$$

$$= 4.2 \text{ MeV}$$

Table 5.1 Beam parameters at treatment plane comparison between chamber and film measurement of single horizontal beam and dual angle beam.

Beam parameters	Chamber measurement		Film measurement	
	Single horizontal beam	Dual angle beam	Single horizontal beam	Dual angle beam
Mean energy ($\bar{E}_0$)	3.3 MeV	3.3 MeV	3.3 MeV	3.4 MeV
Most probable energy ($E_{p,0}$)	4 MeV	4.1 MeV	4.4 MeV	4.2 MeV
D_s	82%	90%	88%	91%
D_{max}	7 mm	6 mm	6 mm	6 mm
R_{50}	14.1 mm	14.3 mm	14.3 mm	14.5 mm
R_p	19 mm	19.5 mm	21 mm	20 mm
D_x	0.3 %	0.2 %	0.9 %	0.4%

The summary of beam parameters at treatment plane from single horizontal beam and dual angle beam are shown in Table 5.1 which compared between parallel plate Roos chamber and film measurement respectively.

Figure 5.8 shows a percentage depth dose curve without degrader compared with degrader in front of treatment plane. The results show that the surface dose of curve without degrader (82%) was less than surface dose of with degrader (90%). Penetration depth of curve without scatterer - degrader was more penetration than using scatterer - degrader. The effect of scatter- degrader was explained by the angular distribution of electron on degrader before reaching the treatment plane that increased surface dose and reduced penetration. The beam parameters are shown in Table 5.2.

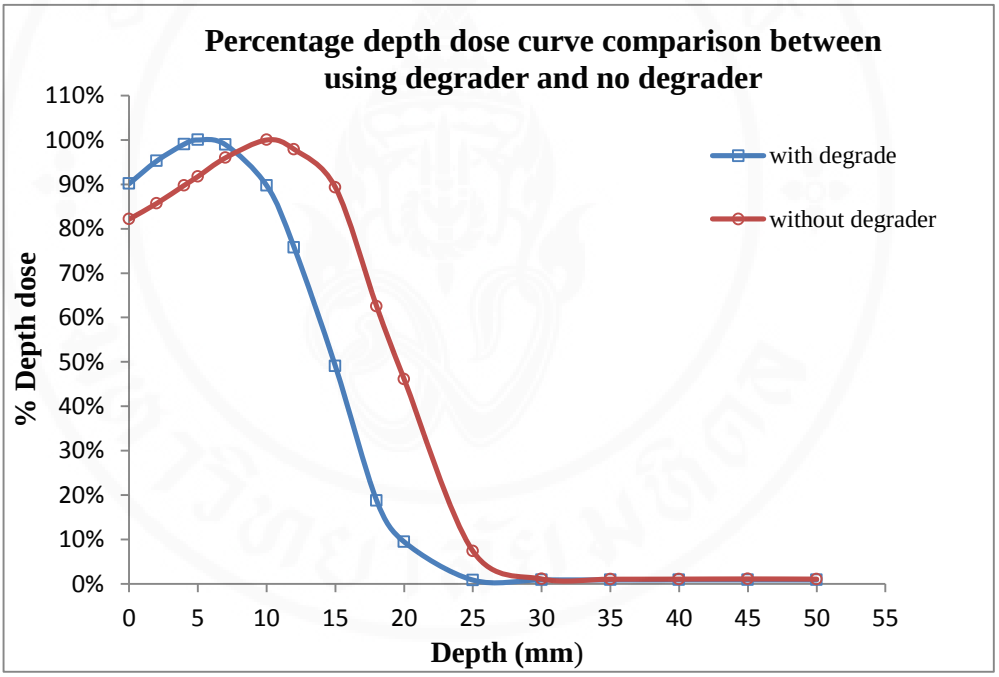

Figure 5.8 Percentage depth dose curve comparison between using scatterer-degrader and no scatterer- degrader measurement by ionization chamber from dual angle beam.

Table 5.2 Beam parameters at treatment plane comparison between using scatterer-degrader and no scatterer- degrader measurement by ionization chamber from dual angle beam.

Beam parameters	Dual angle beam using Roos chamber	
	With scatterer-degrader	Without scatterer-degrader
Mean energy ($\bar{E}_0$)	3.3 MeV	4.4 MeV
Most probable energy($E_{p,0}$)	4.1 MeV	4.9 MeV
D_s	90 %	82 %
D_{max}	6 mm	10 mm
R_{50}	14.3 mm	18.9 mm
Rp	19.5 mm	23.7 mm
Dx	0.3 %	0.5 %

d) Calibration point dose measurement

1) Measurement of calibration point dose following IAEA protocol TRS 398 [7].

The depth at 50% of dose distribution in water (R_{50}) was 1.43 g cm^{-2}

The reference depth in water was calculated from equation (16).

$$Z_{ref} = 0.6(1.43) - 0.1 \quad gcm^{-2}$$

$$= 0.758 \quad gcm^{-2}$$

The conversion of the reference depth in water z_{ref} to reference depth in plastic $z_{ref,pl}$ from equation (17).

$$z_{ref,pl} = 0.758/0.949$$

$$= 0798 \quad gcm^{-2}$$

The Roos chamber was placed on solid water phantom at reference depth $z_{ref,pl}$ 0.8 cm.

The ionization value at depth $z_{ref,pl}$ in phantom ($M_{Q,pl}$) was scaled to ionization value at z_{ref} in water (M_Q) from equation (18).

$$M_Q = 8.3842(nC/1000MU)x1.008$$

$$= 8.4513 \quad nC/1000MU$$

Absorbed dose was calculated following IAEA protocol TRS 398 from equation (19).

$$D_{w,Q} = 8.4513 \frac{nC}{1000MU} x1.0124x1.0015x1.0086x7.9983 \frac{cGy}{nC} x1$$

$$= 0.0691 \quad cGy\ MU^{-1}$$

Absolute dose rate at z_{ref} was converted to that at z_{max} through PDD value from equation (20), PDD at 0.8 cm = 96.55%.

$$D_{w,Q}(z_{max}) = \frac{0.0691 cGy MU^{-1}}{0.9655} x100$$

$$= 0.0716 \quad cGy\ MU^{-1}$$

2) Measurement of calibration point dose following AAPM report 23

The Roos chamber was placed on solid water phantom at a depth of maximum dose (z_{max}) 0.5 cm of solid phantom.

The ionization value at depth z_{max} in phantom ($M_{Q,pl}$) was scaled to ionization value at z_{ref} in water (M_Q) by equation (18).

$$M_Q = 8.7640(nC/1000MU) \times 1.008$$

$$= 8.8341 \quad nC/1000MU$$

Absorbed dose was calculated from equation (19).

$$D_{w,Q} = 8.8341 \frac{nC}{1000MU} \times 1.0131 \times 1.0012 \times 1.0064 \times 7.9983 \frac{cGy}{nC} \times 1$$

$$= 0.0721 \quad cGy\ MU^{-1}$$

Comparison of two measurement protocols.

$$\%\,Different = \frac{0.0721 - 0.0716}{0.0721} \times 100$$

$$= 0.7\ \%$$

The calibration point dose difference between two measurement protocols was less than 1 %. This result represented the matching between IAEA protocol TRS 398 and AAPM report 23. The calibration point dose measured directly at a depth of maximum dose following AAPM report 23 was chosen in this measurement. The HDTse$^-$ mode run at 888 MU/min, so the dose rate at the treatment plane of dual angle fields is approximately 64 cGy /min.

5.2.2 Six dual angle field beam

5.2.2.1 Treatment skin dose measurement

Table 5.3 shows dose value on the surface of cylindrical phantom rotation angle at each 30° intervals. The plot against phantom rotation angle and percent normalized TLD dose which represents the dose uniformity on cylindrical phantom is shown in Figure 5.9. The uniformity was within ± 5% .The treatment skin dose value was 0.194 cGy /MU calculated from the average surface dose on phantom at each 30° intervals.

Table 5.3 TLD dose value (cGy) and relative dose on surface of cylindrical phantom.

Phantom rotation angle (Degree)	TLD dose (cGy/1000MU)	Relative TLD dose (%)
0	183.14 ± 1.86	95
30	191.80 ± 3.70	99
60	203.91 ± 1.08	105
90	201.17± 0.96	104
120	196.14 ± 2.18	101
150	193.22 ± 5.97	100
180	189.19 ± 0.90	98
210	202.51 ± 3.65	105
240	201.08 ± 2.46	104
270	193.13 ± 0.99	100
300	202.84 ± 0.54	105
330	187.40 ± 1.11	97
360	183.14 ±1.86	95
Average	193.59 ± 0.85	100

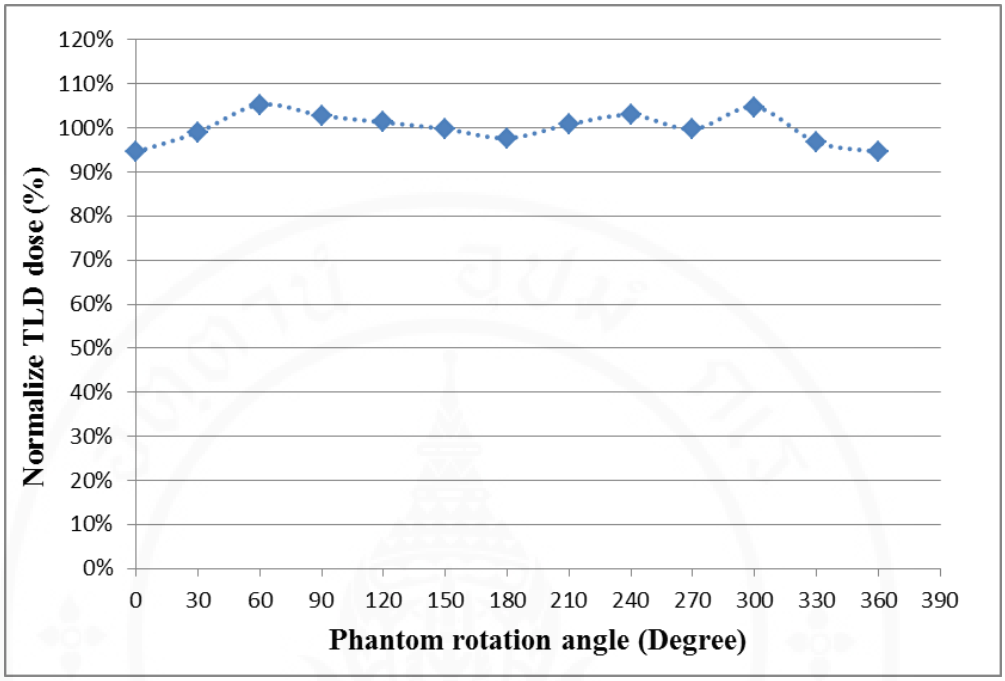

Figure 5.9 Dose uniformity on cylindrical phantom.

5.2.2.2 Overlapping factor (B)

Overlapping factor or factor B is the relation between treatment skin dose (Six dual field beam) to calibration point dose at (0, 0, d_{max}) in the dual field beam.

$$Overlapping\ \ factor = \frac{Treatment\ skin\ dose}{Calibration\ point\ dose}$$

$$= \frac{0.194\,\text{cGy/MU}}{0.0721\,\text{cGy/MU}}$$

$$= 2.69$$

The treatment skin dose was higher than the calibration point dose within range 2.5-3.1 times as recommended in AAPM (23).

MU calculation

$$MU = \frac{\text{Prescribed dose per treatment cycle}}{\text{Output}(cGy/MU) \times B}$$

$$= \frac{200\ cGy\ \text{per treatment cycle}}{0.0721\ cGy/MU \times 2.69}$$

= 1031 MU / Dual angle

~ 516 MU/angle

The treatment time of single angle field is approximately 0.58 min for HDTse $^{-}$ mode (888 MU/min). For a complete treatment cycle, the total treatment time excluding positioning setup is approximately 7 min.

5.2.2.3 Percentage depth dose measurement

Figure 5.10a-5.10c show the exposed film and isodose distribution on three levels of Rando phantom: skull level, chest level and abdomen level (umbilicus level) respectively.

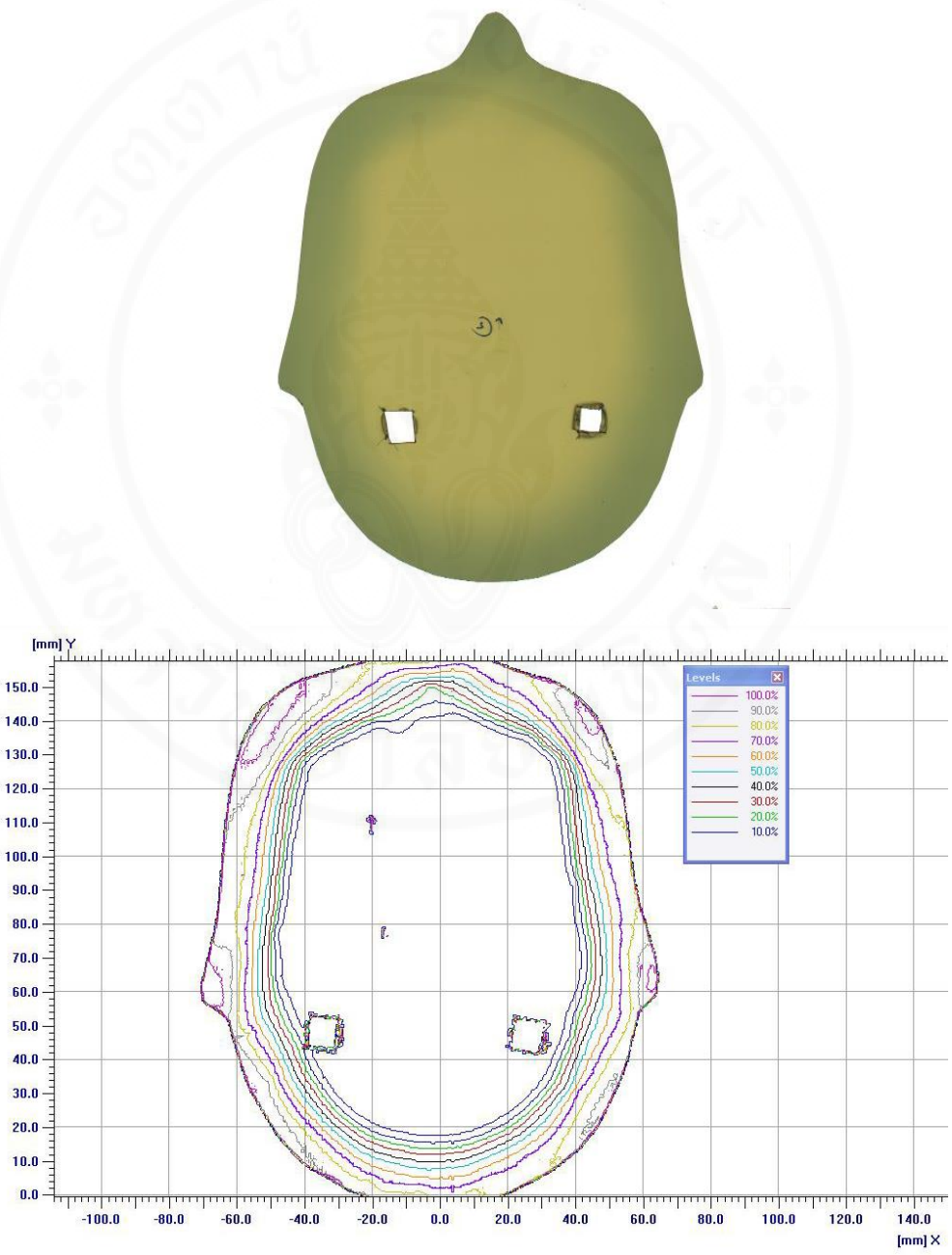

Figure 5.10a The exposed film and isodose distribution on skull level.

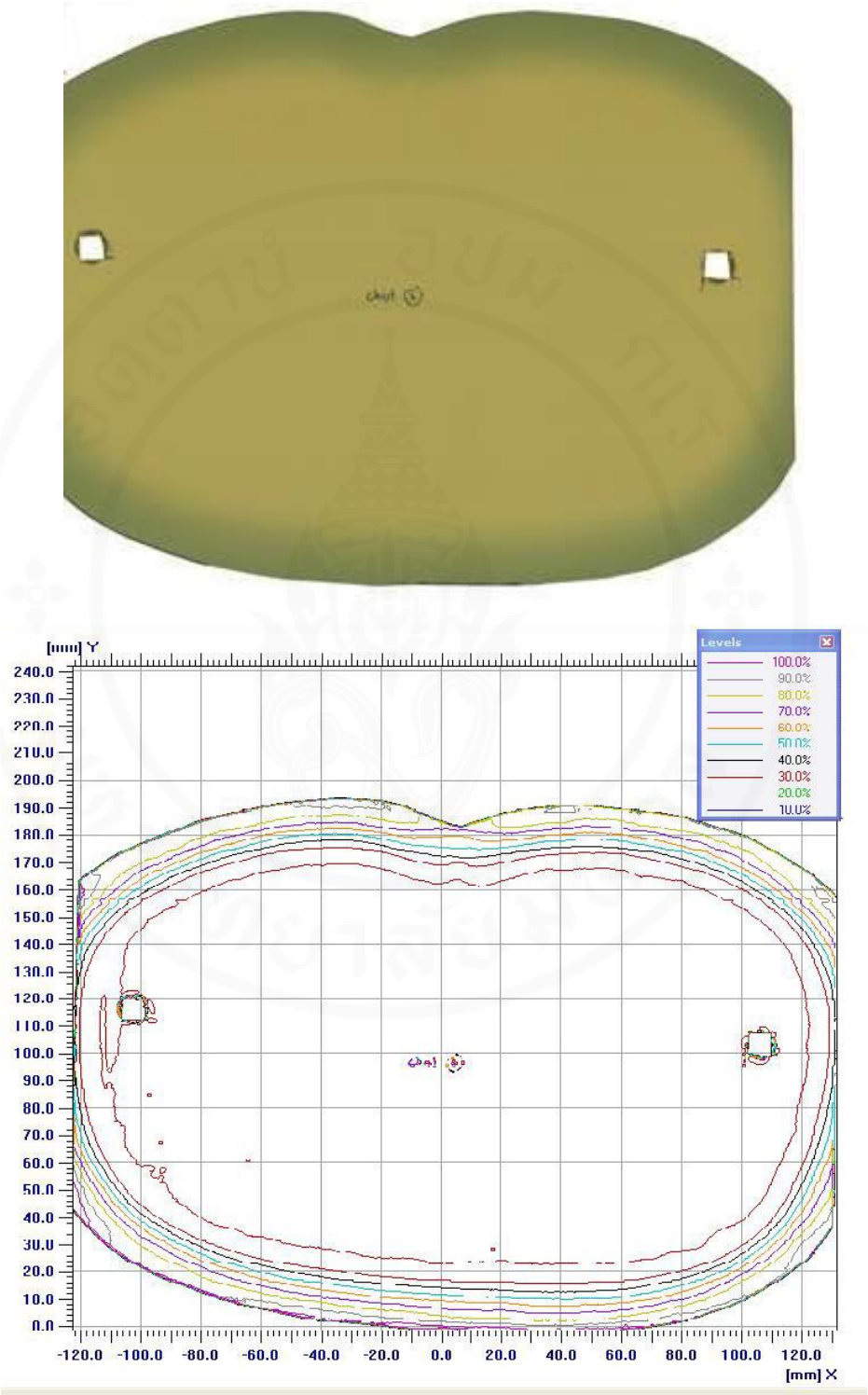

Figure 5.10b The exposed film and isodose distribution on chest level.

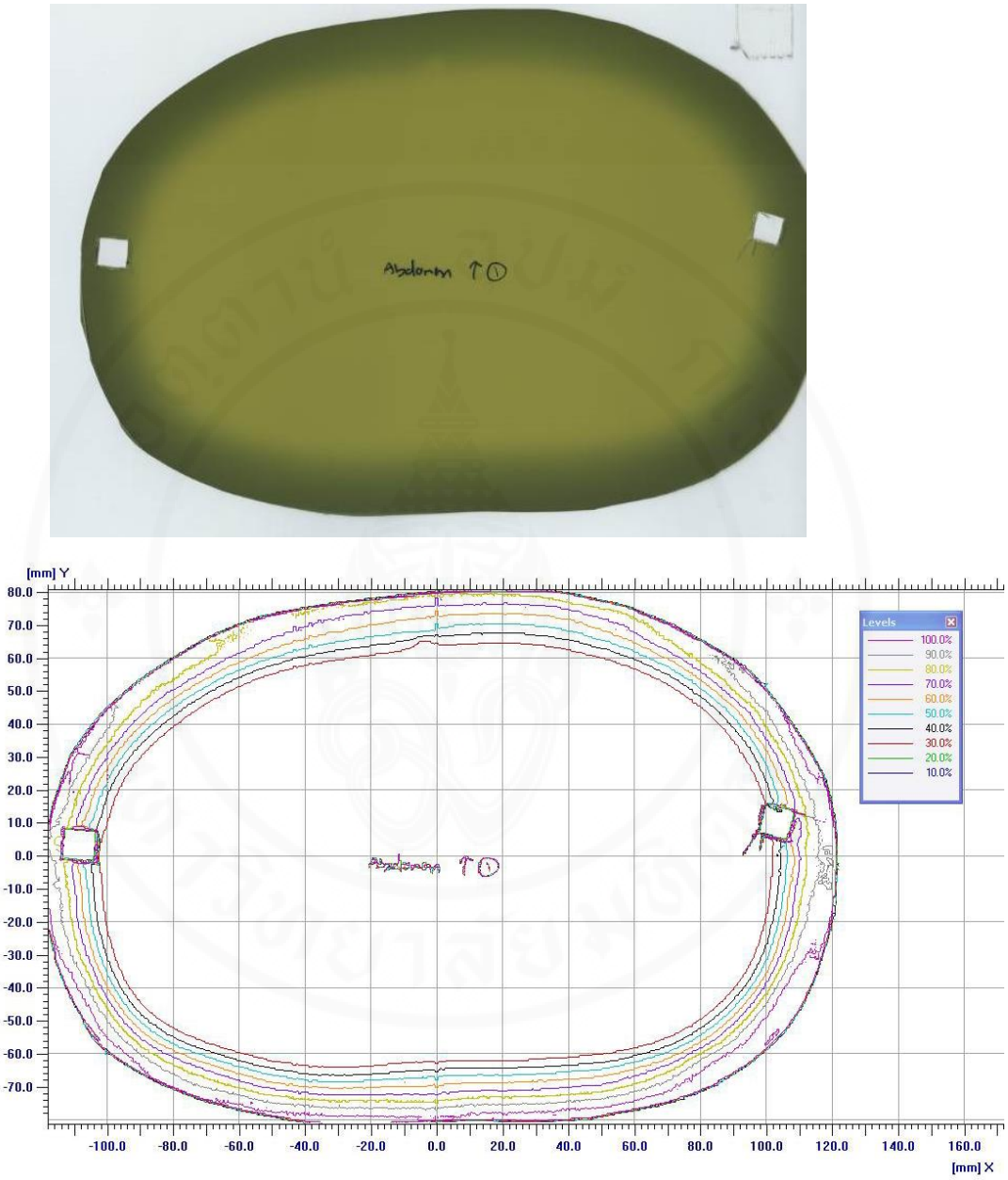

Figure 5.10c The exposed film and isodose distribution on abdomen level.

These Figures show that the opacity of films represented the electron dose from six dual beams. The opacity covered a few centimeters (2-3 cm) on transverse sections of phantom. The isodose distribution also shows isodose lines (10 – 100%) cover a few centimeters which were far away from the axis of the phantom.

Figure 5.11 shows percentage depth dose curve measurement of film on abdomen level slab of Rando phantom from six dual beams compared to that of dual angle beam received from EBT2 measurement. Table 5.4 shows beam parameters at the treatment plane from two percentage depth dose curves on Figure 5.11.

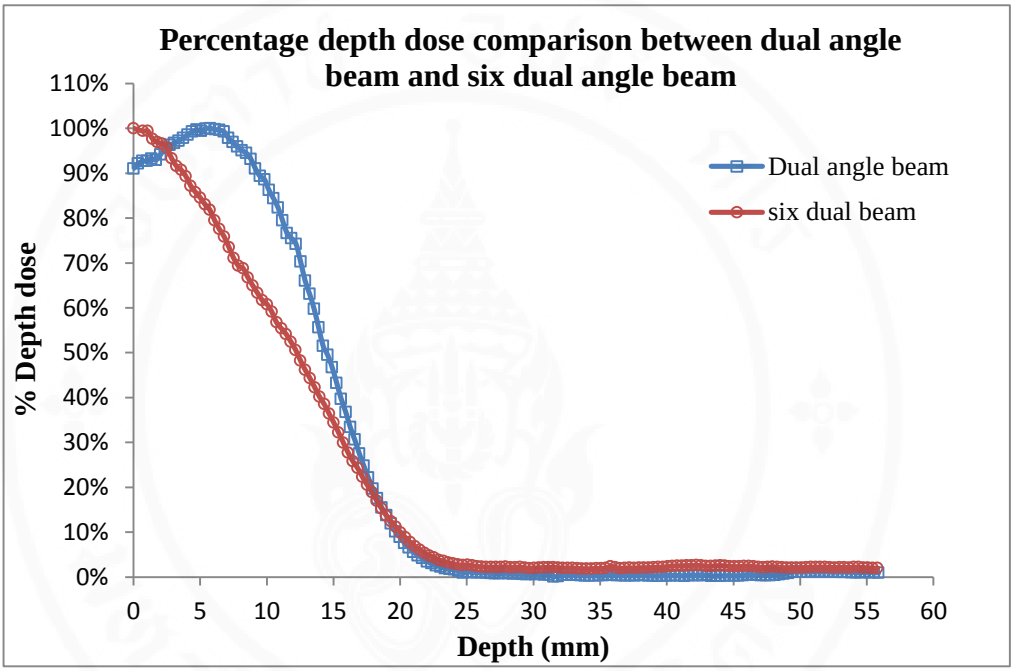

Figure 5.11 Percentage depth dose curve comparison between dual angle beam and six dual angles beams by film measurement.

Table 5.4 Beam parameters at the treatment plane comparison between dual angle beam and six dual angle beam using film measurement.

Beam parameters	Dual angle beam	Six dual angle beam
D_s	91%	100%
D_{max}	6 mm	Surface
D_{80}	11mm	6 mm
R_{50}	14.5 mm	12 mm
D_{20}	17 mm	17 mm
D_x	0.4%	2%

5.2.2.4 Dose uniformity on Rando phantom

Figure 5.12 shows percentage of dose on various point of Rando phantom normalized to the umbilicus point which is the prescription point.

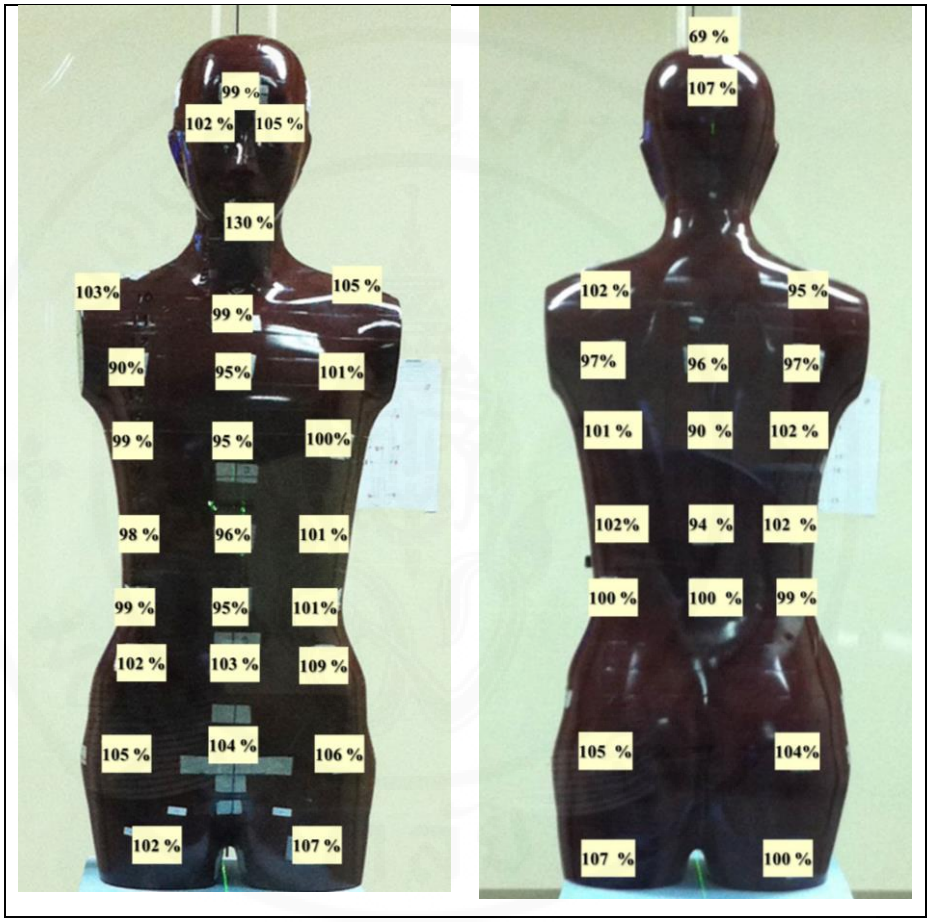

(a) (b)

Figure 5.12 Percentage of dose on various point of phantom
(a) Anterior surface (b) Posterior surface.

Table 5.5 Percent relative surface dose at various points of anthropomorphic phantom surface.

Phantom point	% relative surface dose	Phantom point	% relative surface dose
Vertex	69%	Lt iliac creast	109%
Forehead	99%	Rt femur	102%
Rt eye	102%	Lt femur	107%
Lt eye	105%	Rt medial thigh	52%
Chin	130%	Lt medial thigh	48%
Rt shoulder	103%	Scalp (top rear)	100%
Lt shoulder	105%	Rt temporal	96%
Sternal notch	99%	Lt temporal	104%
Right axilla	90%	Occipital	107%
Mid sternum	95%	Lt scapular	102%
Left axilla	101%	Rt scapular	95%
Rt upper chest	99%	Lt PA chest	97%
Xyphoid	95%	PA chest	96%
Lt upper chest	100%	Rt PA chest	97%
Rt upper abdomen	98%	Lt chest	101%
Upper abdomen	96%	mid line post chest	90%
Lt upper abdomen	101%	Rt thorax	102%
RAO point	99%	Post left abdomen	102%
Center umbilicus	95%	mid abdomen	94%
LAO point	101%	Rt PA abdomen	102%
LPO point	100%	Lt buttock	105%
Posterior point	100%	Rt buttock	104%
RPO point	99%	Lt PA femur	105%
Rt iliac creast	102%	Rt PA femur	102%
Mid iliac creast	103%	Rt head of femur	105%
Pelvis	104%	Lt head of femur	106%

The results of treatment geometry and dosimetry data are discussed as the followings:

- In the whole skin treatment, the extended SSD was used to cover large area. Due to the dimension of the current linear accelerator room, the maximum SSD can be obtained between 3- 4 m SSD which can not be coverd the entire patient (the square field size is between 1.08-1.44 m^2). The combination of beam angulation above and below the horizontal axis called dual angle field was used to solve this [13]. In this study, the SSD of 380 cm was selected which had an approximately field size of 137×137cm^2 from 36 × 36 cm^2 at the isocenter.

- The overlapping of dual angle beam was used to cover and improved dose uniformity along the patient. AAPM23 [4] recommended that the field size must be approximately 200 cm by 80 cm. The vertical uniformity must be within ± 8% and a horizontal uniformity is ± 4 % over 160 cm x 60 cm of treatment plane area. In this study, the ± 18º (72ºand 108º) tilt angle shows the best dose vertical uniformity which has percent relative dose of ± 8% and horizontal uniformity of -3% within 160 cm × 60 cm treatment area. The asymmetry of the upper and lower profile was due to increasing by scattering from the floor. Figure 5.3 shows the same characteristic of the relative dose profile along horizontal axis distance from tilt angle ± 18º, ±19º and 0º respectively. It implies that the tilt angle does not affect in horizontal flatness due to field size in horizontal axis was covered no matter tilt angle used.

- The large scatterer-degrader 0.5 cm thick made of perspex sheet was placed in front of the patient surface at 30 cm distance. This distance was chosen by using vertical beam profile measurement as shown in Figure 5.4. The long distance of degrader from treatment plane will affect to lower dose on the upper profile due to scatter from air to treatment plane. Figure 5.8 shows a percentage depth dose curve without scatterer-degrader compared with scatterer - degrader in front of treatment plane. The results show that the surface dose of curve without scatterer- degrader was less than surface dose of with degrader. Penetration depth of curve without scatterer - degrader was more penetration than using scatterer - degrader. The scatterer - degrader has a property by its name that scattering or broadening electron beam to improve dose uniformity and degrading the energy by reducing the depth of penetration. El –Khatib et al. [22] studied the beam penetration with and without

scatterer- degrader on six dual beam. The results showed that without scatterer-degrader the desired beam penetration could not be produced. The effect of scatter-degrader was explained by the angular distribution of electron on degrader before reaching the treatment plane that increased surface dose and reduced depth of penetration.

- Percentage depth dose curves compared between single horizontal beam and dual angle beam. The result showed that two curves almost superimposed corresponding in both chamber and film measurement. The surface dose of dual angle beam was slightly increased from 88 % for the single horizontal beam to 91 % for dual angle beam due to oblique incidence of the electron beam by beam angulation. This effect increases dose to the surface and shift depth of maximum dose (d_{max}) toward the surface.

- The x- ray contamination of single horizontal beam was higher than dual angle beam because of the characteristic of x-ray is penetrating in forward direction [13,14]. Therefore angling beam above and below the body can reduce the x-ray contamination to the patient.

- Table 5.1 shows the beam parameters at treatment plane comparison between chamber and film measurement of dual angle beam. The maximum dose was laid at a depth of 6 mm and dropped to 50% dose at a depth of 14.3 mm and 14.5 mm from chamber and film measurement respectively. The x- ray contamination was less than 1% at a depth of 2.5 cm corresponding in both chamber and film. The initial electron energy of 6 MeV was reduced to the most probable energy 4.1 MeV and the mean energy about 3.3 MeV when it's traveling in the air and passing through scatterer - degrader. The x-ray contamination was about 0.4 %.

- The calibration point dose was measured at a depth of maximum dose using parallel plate Roos chamber following AAPM 23 protocol. The TRS-398 protocol [7] was also used to compare with the earlier protocol. The results show the agreement with two protocols. The difference was less than 1 %. The calibration point dose measure directly at d_{max} following AAPM report 23 was chosen in this study. This result was consistent with the study by P. Schiapparelli et al. [28] They also observed that Roos chamber had no evident cable effect of different length irradiated cable. There was no need to shield the cable during measurement. The calibration

point dose was 0.0721cGy/MU at d_{max} for dual angle fields. The HDTse $^{-}$ mode run at 888 MU/min, so the dose rate at the treatment plane of dual angle fields is approximately 64 cGy/ min.

- For six dual angle field beams, the treatment skin dose on the surface of the cylindrical phantom rotation angle at each 30º intervals using TLD measurement was 0.194 cGy /MU. The relation of treatment skin dose to calibration point dose from a dual angle beam called overlapping factor B was equal to 2.69 which was in the range of 2.5 -3.1 as recommended in AAPM report 23. Its result was from the three dual fields contributing to each point. It was used to specify the monitor units for each field. A prescription dose of 200 cGy was given in one complete treatment cycle of six dual field beam corresponding to 516 MU for each of angle field (twelve angle fields).

- The percentage depth dose curve for the complete treatment cycle was measured on transverse sections of an anthropomorphic phantom by EBT2 film. The results show that the depth of maximum dose was shifted to surface and depth of penetration was decreased compared with one dual angle beam. The dose falls off to 80 % of maximum dose at 6 mm depth, 50% of maximum dose at 12 mm depth and the 20 % of maximum dose at 17 mm depth. The x- ray contamination of six dual beams beyond 30 mm depth was increased to 2 % that was also caused by the combination of multiple beams. Moreover, the x- ray contamination also measured using TLD-100 chips placed in the hole of an anthropomorphic phantom and compared with that of EBT2 film result. It has 0.8 % x-ray contamination compared to 2 % result from EBT2 film measurement. The higher results of EBT2 film measurement explain by the error in low dose measurement of EBT2 film (dose < 0.25 cGy) as shown in appendices table B.1.

- The percentage depth dose of the complete treatment cycle in this study were corresponding to the recommendations of EORTC [2] (80% isodose) which is at least 4 mm depth, and the dose at 20 mm depth should be less than 20% of maximum dose. The x- ray contamination meets the AAPM23 suggestion of a 4 % x-ray contamination (~1.5 cGy). However it is unsatisfied in the clinic.

- For in vivo dosimetry, TLD-100 chips in plastic bag were taped on various points of phantom surface. The percentage dose were varies from 48% to 130%. The highest percentage dose was at the chin surface which received multiple

beams and oblique beams in the treatment. The lowest percent dose is at the medial thigh which is in the inner area (inner thigh). This area cannot be received the proper beam due to the anatomy site. The vertex surface is also has a low percentage dose (69%) due to the anatomy site which received only scatter beam. The underdose areas must be boost later in order to receive an adequate dose in the treatment. Some studies had been designed by putting the lead sheet above the scalp to scatter the dose to the vertex [30].The percentage dose on the trunk was between 90% - 109% corresponding with many literatures [25, 31, 32]. The results showed that the uniformity of this treatment technique was within ±10%. However these results were received from phantom measurement. For the patient, the dose uniformity was varied more than ±10%. Anacak et al. [25] studied in vivo dosimetry on 67 TSEI treatment founded that dose uniformity throughout the skin surface is 15% compared with humanoid phantom The uniformity at the trunk was better than the extra-trunk which were mobile parts of the body. It was due to the shape, curvature and orientation of the body surface to the beam. Many studies recommended that the in vivo dosimetry such as TLD dosimetry [25,31,32] and film dosimetry [33,34] measured on various points of the patient during the treatment are still absolutely necessary in order to verify the prescribed dose and dose uniformity.

CHAPTER VI
CONCLUSIONS

All dosimetric parameters of Modified Stanford technique using an electron energy 6 MeV high dose rate mode on a linac Varian Clinac iX at Ramathibodi hospital have been measured according to AAPM23 guidelines. The followings are my study's conclusions.

6.1 The advantage of high dose rate mode is desirable for shortening the treatment time. The standing patient can tolerate during the treatment.

6.2 The electron energy at treatment plane was reduce from 6 MeV to 3.4 MeV. It was due to the extended SSD (380 cm) and the angular distribution of nominal electron on scatterer - degrader before reaching the treatment plane.

6.3 All dosimetric parameters have met the requirement for TSEI treatment. R_{80} was 6 mm depth and the D_{20} was 17 mm which were corresponding to the recommendations of EORTC.

6.4 The x-ray contamination was about 2 % which were corresponding to the recommendations of AAPM23 (1-4%).

6.5 The uniformity on the trunk was within ±10%. These results were coming from phantom measurement which met the criteria of the uniformity.

Above all, the in vivo measurement is an important procedure to verify the dose uniformity around the patient's surface which is the main objective of the treatment. Additionally, the boosted area and shielding area must be known exactly for treatment. The shielding areas such as eyes, scalp, fingers and feet. Boosting areas such as perineum and soles.

The further study is the verification of patient dose during the treatment using thermoluminescent dosimeters and diode dosimeters.

REFERENCES

1. Khan FM .The physics of radiation therapy 3nded, Philadelphia: Lippincott Williams and Wilkins; 2003.
2. Jones GW, Kacinski BM, Wilson LD, Willemze R, et al. Total skin electron radiation in the management of mycosis fungoides: consensus of the European organization for research and treatment of cancer (EORTC) cutaneous lymphoma project group. J Am Acad Dermatol, 2002; 47(3), 364-370.
3. Lynn DW, Ginette AH, James BY. Age, Race, Sex, Stage, and Incidence of Cutaneous Lymphoma.Clin Lympho 2012; 12(5):291-296.
4. Karzmark CJ, Anderson J, Buffa J, Fessenden P, Khan FM, et al. Total skin electron therapy: Technique and dosimetry, AAPM Radiation Therapy Committee Task Group 30, Report No. 23, 1987.
5. International Commission on Radiation Units and Measurements. Radiation dosimetry: Electron with initial energies between 1 and 50 MeV.Washington DC : ICRU Report 35,1984;15:1-157.
6. Khan FM, Dopple KP, Hongstorm KR, et al. Clinical electron dosimetry : Report of AAPM Radiation Therapy Task Group No 25. Med Phys 1991; 18(1):73-108.
7. Andreo P, Burns DT, Hohfeld K, Huq MS, Kanai T, Laitano F, Smyth VG, Vynckier. Absorbed dose determination in external beam radiotherapy: An international code of practice for dosimetry based on standards of absorbed dose to water IAEA Technical Report Series No 398. Austria: IAEA publication; 2000.
8. Steven MH, Elise AO, Madeleine D, et al. Review of the treatment of mycosis fungoides and sezary syndrome: a stage-based approach. J NCCN 2008; 6(4):436-442.
9. Stephen LM. Skin lymphoma. Clin, oncol 2012; 24:371-385

10. Scholtz W.Uber den einfluss der roentgenstrohlem auf diehaut in gesundem und krankem zustande. Arch Dermatol Syph 1902; 59:421-446.
11. Sommerville J. Mycosis fungoides treated with general X-rays bath. Br J Dermatol 1939; 51: 323-324.
12. Trump JG, Wright KA, Evans WW, et al. High energy electrons for the treatment of extensive superficial malignant lesions. AJR1953; 63: 623-629.
13. Karzmark CJ, Loevinger R, Steele RE, et al. A technique for large-field superficial electron therapy. Radiol 1960; 74: 633-643.
14. Page V, Gardner A, Karzmark CJ. Patient dosimetry in the electron treatment of large superficial lesions. Radiol.1970; 94: 635-641.
15. Kumar PO, Patel Is. Rotation technique for superficial total body electron beam irradiation. J Natl Med Assoc 1978; 70:507-509.
16. Williams PC, Hunter RD, Jackson SM . Whole body electron therapy in mycosis fungoides a successful translational technique achieved by modification of an established linear accelerator British Journal of Radiology 1979; 52: 303.
17. WU JM, Leung SM, Wang CJ et al. Lying-on position of total skin eletron therapy. Int J Radiant Oncol Biol Phys 1997; 39(2): 521-528.
18. WU JM, Yeh SA,Hsiao KY. A conceptual design of rotating board technique for delivering total skin electron therapy Med Phys 2010; 37:1449-1458.
19. Shouman T, El-Tahel Z. Total skin electron therapy: a modisied technique for small room linear accelerator. J Egypt Natl Canc Inst 2004;16(4):202-209.
20. Podgorsak EB. , Podgorsak MB. Radiation Oncology Physics: A handbook for teachers and students. Austria : IAEA publication ; 2005.
21. Reynard EP, Evans M, Devic S, Parker W, Freeman CR, Roberge D, Podgorsak EB. Rotational total skin electron irradiation with a linear accelerator. J Appl Clin Med Phys 2008; 9(4): 404.
22. el-Khatib E, Hussein S, Nikolic M, Voss NJ, Parsons C.Variation of electron beam uniformity with beam angulation and scatterer position for total skin irradiation with the Stanford technique. Int J Radiat Oncol Biol Phys.1995; 33(2):469–474.

23. International Commission on Radiation Units and Measurements, Tissue substitutes in radiation dosimetry and measurement. Bethesda,MD, ICRU Report 44, 1989.

24. Fraass BA, Robinson PL, Glatstein E. Whole-skin electron treatment patient skin dose distribution. Radiol 1983; 146 :811-814.

25. Anacak Y, Arican Z, Deroma RB,Tamir A, Kuten A. Total skin electron irradiation: Evaluation of dose uniformity throughout the skin. Med Dos 2003; 28(1): 31-34.

26. Das IJ, Copeland JF, Bushe HS. Spatial distribution of bremsstrahlung in dual electron beam used in total skin electron treatments: Errors due to ionization chamber cable irradiation. Med.Phys 1994;21(11):1733 - 1738.

27. Harshaw Bicon.Model 5500 automatic TLD reader user's manual. Ohio: Saint-Gobain/Norton Industrial Ceramics Corporation;1993

28. Schiapparelli P, Zefiro D, Massone F, Taccini G. Total skin electron therapy (TSET): A reimplementation using radiochromic films and IAEA TRS-398 code of practice. Med Phys 2010; 37(7):3510 – 3517.

29. Cox RS, Heck RJ, Fessenden P, Karzmark CJ, Rust DC. Development of total-skin electron therapy at two energies. Int J RadiatOncol Biol Phys 1990; 18(3): 659-669.

30. Peter VG. Use of an electron reflector to improve dose uniformity at the vertex during total skin electron therapy. Int J Radiat Oncol Biol Phys 2000; 46(4): 1065-1069.

31. Weaver RD, Gerb BJ, Dusenbery KE et al. Evaluation of dose variation during total skin electron irradiation using Thermoluminescent dosimeters. Int J Radiat Oncol Biol Phys 1995; 33(2):475-478.

32. Antolak JA, Cundiff JH and Chul S Ha.Utilization of thermoluminescent dosimetry in total skin electron beam radiotherapy of mycosis fungoides. Int. J. Radiat. Oncol. Biol. Phys 1998; 40(1):101-108.

33. Bufacchi A, Carosi A, Adorante N, et al. In vivo EBT radiochromic film dosimetry of electron beam for Total Skin Electron Therapy(TSET). Physica Medica 2007; 23(2):67-72.

34. GambleLM, Farrell TJ, Jones GW et al. Two-dimensional mapping of underdosed areas using radiochromic film or patients undergoing to skin electron beam radiotherapy. Int J Radiat Oncol Biol Phys 2005; 62(3):920-924.

APPENDICES

APPENDIX A

1.Calibration of thermoluminescence dosimeter

1.1 TLD-100 calibration

TLD must be calibrated with known dose in the same type of energy that used in the measurement before using. The processes were

(i) TLD chips 150 chips were annealed in heat temperature 400 °C for 1 hour and100 °C for 2 hours in order to clear the remaining signal.

(ii) The TLDs were placed in the perspex plate under bolus thickness 1.4 cm at SSD 100 cm, cone size 15 x 15 cm^2 and irradiated by the electron beam energy 6 MeV for radiation dose 2 Gy

(iii) Preheating the irradiated TLDs at heat temperature 100 °C for 10 minutes before reading by TLD reader .Then preheated TLDs were read in nanocoulombs (nC)

(iv) Following (i) - (iii) for 3 times .Then averaging the value of individual TLD. The average values were compared with the mean value. If the difference is more than 10 %, those TLDs were rejected.

(v) The Element Correction Coefficient (ECC_i) for each TLD were calculated from equation:

$$ECC_i = \frac{\bar{Q}}{Q_i} \quad (1)$$

Where $\bar{Q}$ is the average value of all TLDs

Q_i is the individual value of each TLD

(vi) The eight TLDs that had the ECC_i values close to 1 were chosen.

There were the standard TLDs for the calibration. Then the eight standard TLDs were irradiated following (i) - (iii) for 2 times. Calculated the corrected charge integral (Q_{ci}) from equation:

$$Q_{ci} = Q_i x ECC_i \quad (2)$$

Where Q_i is the average value of each standard TLDs.

(vii) The Q_{ci} of each standard TLDs was averaged and then calculated Reader Calibration Factor (RCF) for the whole set of the standard TLDs

$$RCF = \frac{\bar{Q}_c}{D} \quad (3)$$

Where $\bar{Q}_c$ is average value of the ten standard TLDs

D is the irradiated radiation dose 2 Gy

(viii) For the rest of TLDs (140 TLDs) or field TLDs were irradiated following (i) - (iii) for 2 times and then calculated the calibration value or element correction coefficient of each TLD from equation :

$$ECC_{ci} = \frac{RCF x D}{Q_i} \quad (4)$$

Then each field TLD had its ECC_{ci} . They were ready for measuring the unknown dose (D_u) by using an equation:

$$D_u = \frac{Q_i x ECC_i}{RCF} \quad (5)$$

Where Q_i is the individual value of each field TLD

The Element Correction Coefficient (ECC_i) value for each TLD were shown in Table A.1. The value varied from 0.7908 to 1.2840 that were within acceptable range (0.7-1.3) as recommended in the manual [27].

The reader calibration factor (RCF) calculated from eight standard TLDs in equation (3) was 1.0343×10^3 nC/Gy. The ECC_{ci} was the calibration value for 110 field TLDs that used to convert the reading of a field TLD to unknown dose (D_u). The values varied from 0.7779 to 1.3069 were rearranged and shown in Table A.2.

Table A.1 The element correction coefficient (ECC_i) value for each TLDs.

TLD No	ECC_i	TLD No	ECCi	TLD No	ECCi	TLD No	ECCi
2	1.0024	34	1.1178	67	0.8388	100	1.2652
3	1.2242	35	0.9032	68	1.2692	101	0.8767
4	1.0323	36	0.8167	69	1.2062	102	0.8570
5	0.7934	37	1.0730	70	1.0226	104	0.8498
6	0.8809	38	0.9048	71	0.9892	105	0.9005
7	1.0273	39	1.2195	72	1.0586	106	0.8132
8	0.8979	40	1.2477	73	1.1446	107	0.9461
9	1.0165	41	1.2612	74	1.0593	108	0.9198
10	1.0422	42	1.1166	75	1.1082	109	0.8817
11	0.8790	43	0.9471	76	0.9674	110	1.1390
12	0.9036	44	1.0015	77	0.9607	112	1.0380
13	0.9056	45	1.1498	78	1.1476	113	0.9993
14	1.0713	46	0.8422	79	0.8173	114	0.9051
15	0.9341	48	1.2245	80	0.8243	115	0.9695
16	0.8933	49	1.1748	82	1.2130	116	1.0057
17	0.9250	50	1.0858	84	0.9144	117	1.0003
18	0.9804	51	0.8802	86	1.0093	118	1.1777
19	1.0888	53	0.8691	88	0.9271	119	1.0931
20	1.1819	54	1.2840	89	1.0469	120	0.8428
22	1.1781	55	1.1370	90	0.8915	123	1.0026
23	0.8705	56	0.9606	91	1.2735	124	1.0243
24	0.9817	57	1.2824	92	1.0608	125	1.1533
25	1.0375	58	0.9776	93	1.1811	127	0.9140
26	1.2106	59	1.0709	94	1.0127	128	0.9430
27	1.0636	61	1.0561	95	0.9680	129	0.9849
28	1.0375	62	0.8487	96	0.8551	131	0.9959
30	1.1466	63	1.1325	97	0.8852	132	0.9876
31	0.9635	64	1.1541	98	0.9234	133	0.7908

Table A.1 The element correction coefficient (ECC_i) value for each TLD (cont.).

TLD No	ECCi	TLD No	ECCi	TLD No	ECCi	TLD No	ECCi
32	0.8187	65	1.0919	99	0.9495	135	0.9384
33	1.2019	66	1.1374				

Table A.2 The element correction coefficient (ECC_{ci}) for each TLD.

TLD No.	**$ECCc_i$**	**TLD No.**	**ECCci**	**TLD No.**	**ECCci**	**TLD No.**	**ECCci**	**TLD No.**	**ECCci**
1	1.2155	23	1.1917	45	0.8980	67	1.1410	89	0.8733
2	1.0412	24	1.0734	46	0.8890	68	0.9904	90	0.9065
3	0.7905	25	1.0415	47	1.3070	69	0.9997	91	0.8036
4	0.8897	26	1.1097	48	1.1451	70	1.1690	92	0.9312
5	1.0270	27	1.0032	49	0.9840	71	0.8009	93	0.9282
6	0.8987	28	0.7997	50	1.3056	72	0.8205	94	0.8771
7	1.0178	29	1.2005	51	0.9836	73	1.2141	95	1.1317
8	1.0075	30	1.1192	52	1.0847	74	0.9136	96	1.0102
9	0.8815	31	0.8841	53	1.0486	75	0.9565	97	0.8861
10	0.9053	32	0.7850	54	0.8387	76	1.0613	98	0.9475
11	0.9195	33	1.0765	55	1.1719	77	0.9125	99	1.0543
12	1.0622	34	0.8801	56	1.1445	78	1.2589	100	1.0368
13	0.9491	35	1.2146	57	1.1179	79	1.0151	101	1.1827
14	0.9421	36	1.2439	58	1.1661	80	1.1794	102	1.0739
15	0.9303	37	1.2772	59	0.8506	81	0.9718	103	0.8303
16	0.9791	38	1.1252	60	1.2772	82	0.8495	104	0.9962
17	1.1172	39	0.9447	61	1.2102	83	0.8661	105	1.1868
18	1.2017	40	1.1234	62	1.0227	84	0.9187	106	0.9071
19	1.1450	41	0.8339	63	0.9503	85	0.9443	107	0.9679
20	0.8690	42	1.1951	64	1.0504	86	1.2616	108	0.9862
21	0.9803	43	1.1700	65	1.1879	87	0.8860	109	0.7779
22	1.0545	44	1.1019	66	1.1003	88	0.8558	110	0.9429

1.2 Linearity test of the TLD-100

After calibration, the linearity of all TLDs was tested .The process was:

(i) All TLDs were placed in the Perspex phantom under bolus thickness 1.4 cm at SSD 100 cm , cone size 15 x 15 cm^2 and irradiated by the electron beam energy 6 MeV with known doses 0.25 Gy

(ii) All TLDs were read by automatic TLD reader and then calculated average TLD values (nC)

(iii) Following (i) - (ii) with doses 0.5 Gy,0.75 Gy,1 Gy 2 Gy and 2.5 Gy

(iv) The plot against irradiated dose and average dose measurement by the TLDs was shown in Figure A.1. The curve shows a linear relation with a correlation coefficient $R^2 = 0.9997$

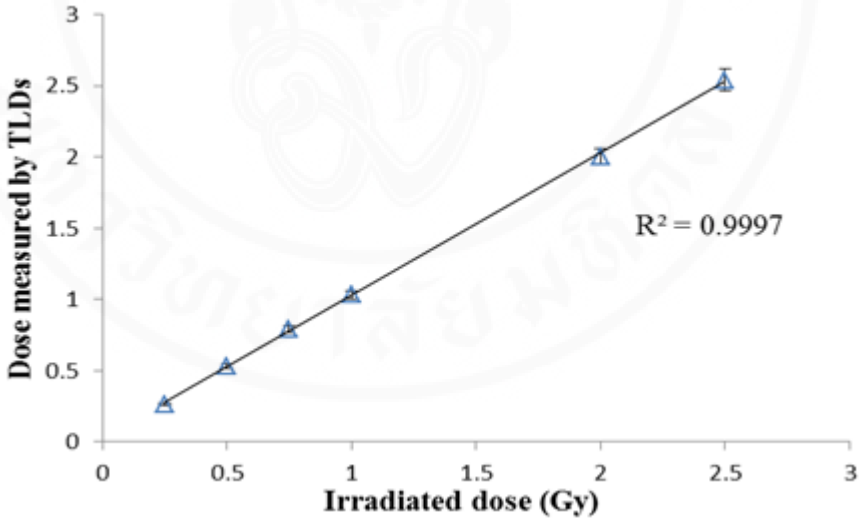

Figure A.1 The linearity of TLDs.

APPENDIX B

Calibration of film

GAFCHROMIC ® EBT2 film size 8" x 10" (lot #A08111102, expired on Aug 2013) was used in this measurement. Film calibration was performed for defining the relationship between the net optical density and absorbed dose.

The film sheet was cut into 3 x 3 cm^2 for 24 pieces on the day of irradiation and stored in an opaque package in order to protect the film from visible light. Each film sheet was placed on solid water phantom 15 cm thickness (to provide backscatter) perpendicular to the central axis of the beam. Each film was irradiated by the electron beam energy 6 MeV with cone size 15 x15 cm^2 at a depth of maximum dose of electron energy 6 MeV (1.4 cm), 100 cm SSD with known dose ranges from 5 cGy to 800 cGy. After 24 h irradiation, all films were scanned by Vidar scanner with resolution of 72 dpi and color depth of 16 bit depth. The image was saved in TIFF format and analyzed by ImageJ. The calibration curve was plotted against pixel value and known dose. The dose conversion from pixel value to dose was fitted with a second level of polynomial function using Microsoft excel.

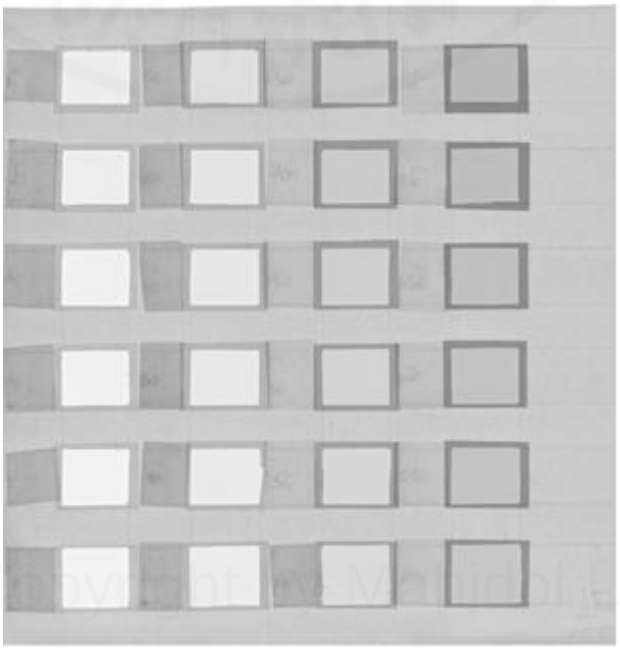

Figure B.1 Film calibration of electron energy 6 MeV with 24 dose levels.

Table B.1 The percent difference between calculated dose and irradiated dose of film calibration.

Level	Irradiated dose (cGy)	Pixel value	Calculated dose (cGy)	%Diff
1	0	3059	-0.23	-
2	5	3572	8.22	64%
3	10	3806	12.51	25%
4	15	4078	17.86	19%
5	25	4469	26.20	5%
6	30	4757	32.85	9%
7	40	4905	36.42	-9%
8	50	5325	47.19	-6%
9	60	5680	56.98	-5%
10	80	6330	76.58	-4%
11	100	6918	96.17	-4%
12	150	8301	149.17	-1%
13	200	9367	196.67	-2%
14	250	10455	251.12	0%
15	300	11297	297.39	-1%
16	350	12330	359.10	3%
17	400	13076	407.04	2%
18	450	13776	454.59	1%
19	500	14277	490.17	-2%
20	550	15104	551.68	0%
21	600	15720	599.76	0%
22	650	16297	646.55	-1%
23	700	16986	704.65	1%
24	800	18012	795.63	-1%

Table B.1 shows the results of dose conversion using dose conversion from pixel value of calibrated EBT2 films 24 dose level. Figure B.2 shows the calibration curve for EBT2 film irradiated with electron energy 6 MeV. The pixel values were plotted against dose ranges from 0 cGy to 800 cGy. The dose conversion from pixel value to dose was fitted to a second order polynomial and the linear correlation coefficient values (R^2) was 0.9997.

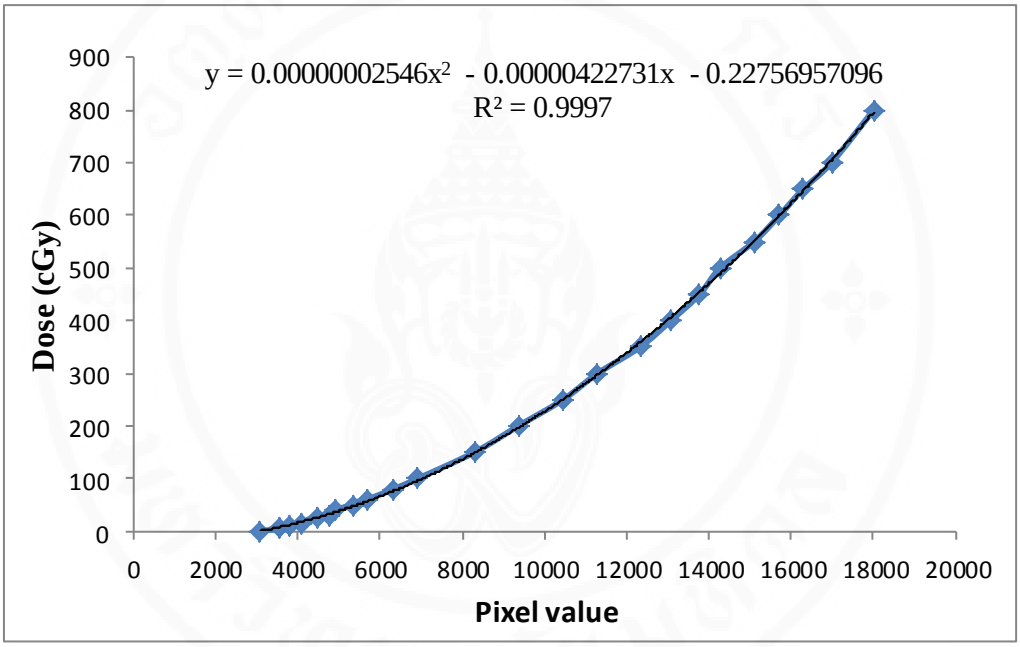

Figure B.2 Calibration curve of EBT2 film for a 6 MeV electron beam , 15 x 15 cm^2 cone at d_{max} 1.4 cm , 100 cm SSD.

BIOGRAPHY

NAME	Miss. Supaporn Srisuwan
DATE OF BIRTH	12 March 1983
PLACE OF BIRTH	Chumphon, Thailand
INSTITUTIONS ATTENDED	Mahidol University, 2004: Bachelor of Science (Radiological Technology) Mahidol University, 2013: Master of Science (Medical physics)
RESEARCH GRANTS	Graduate Studies of Mahidol University Alumni Association
HOME ADDRESS	163 Moo 5, Thayang, Aumphor Mueng, Chumphon, Thailand 86000 Tel. 086-5225427 E-mail: supaporn.srs@mahidol.ac.th
EMPLOYMENT ADDRESS	270 Ramathibodi Hospital, Rama 6, Payathai, Bangkok, Thailand 10400 Tel. 0-22011657 E-mail: supaporn.srs@mahidol.ac.th
PUBLICATION / PRESENTATION	13th Asia-Oceania Congress of Medical Physics & 11th South-East Asian Congress of Medical Physics